

# Evaluation of corrosion inhibition capability of graphene modified epoxy coatings on reinforcing bars in concrete

Nikhil Sharma <sup>a,\*</sup>, Shruti Sharma <sup>b</sup>, Sandeep K. Sharma <sup>c</sup>, Roop L. Mahajan <sup>d,e</sup>, Rajeev Mehta <sup>f</sup>

<sup>a</sup> Research Scholar, TIET-VT Center of Excellence in Emerging Materials (CEEMS), Civil Engineering Department, Thapar Institute of Engineering & Technology, Patiala 147004, India

<sup>b</sup> Affiliate Faculty, TIET-VT Center of Excellence in Emerging Materials (CEEMS) & Professor, Civil Engineering Department, Thapar Institute of Engineering & Technology, Patiala, India

<sup>c</sup> Affiliate Faculty, TIET-VT Center of Excellence in Emerging Materials (CEEMS), Associate Professor, Mechanical Engineering Department, Thapar Institute of Engineering & Technology, Patiala, India

<sup>d</sup> Lewis A Hester Chair Professor, Department of Mechanical Engineering, Virginia Tech, Blacksburg, USA

<sup>e</sup> Chair Professor, TIET-VT Center of Excellence in Emerging Materials (CEEMS), Thapar Institute of Engineering & Technology, Patiala, India

<sup>f</sup> Coordinator, TIET-VT Center of Excellence in Emerging Materials (CEEMS), Professor and Head, Chemical Engineering Department, Thapar Institute of Engineering & Technology, Patiala, India

## ARTICLE INFO

### Keywords:

Corrosion  
Graphene oxide  
Reduced graphene oxide  
Carbon nano-tubes (CNT)  
Corrosion current  
Ultrasonic guided waves  
Reinforced concrete  
Silane agents

## ABSTRACT

Corrosion of reinforced concrete structures is the one of the biggest problems faced by the construction industry, with billions of dollars spent annually on corrosion control strategies. Epoxy Coated Rebars (ECRs) have been reported to mitigate corrosion in Reinforced Concrete (RC) structures, but due to the inherent brittle nature of epoxy, its usage is limited. In this study we have proposed modified epoxy coatings on rebars using reduced graphene oxide (rGO) and graphene oxide (GO) along with carbon nanotubes (CNTs) and silane agents for improved ductility and corrosion inhibition properties. Hybrid mixture of CNTs and rGO/GO enhances the mechanical strength of the coating matrix whereas silane agents improve dispersion and bonding characteristics of nano fillers. Differently coated mild steel rebars with rGO/GO based coatings were subjected to accelerated impressed current corrosion. Performance of the coatings was evaluated by visual inspection, corrosion current, ultrasonic guided wave measurements, mass loss and residual tensile strength. Our results indicate that compared to rGO, GO in small proportion (0.4 wt% of epoxy resin) performs superior in corrosion inhibition. The GO/CNT nano composites could have potential application in the field of modified ECR reinforced concrete structures.

## 1. Introduction

Corrosion of civil infrastructures is the biggest challenge faced by the construction industry worldwide, and it is estimated that billions of dollars are spent for their repair and rehabilitation. About \$2.5 trillion USD is the global cost of the corrosion related maintenance and repairs strategies in all industries [1,2]. Over \$ 100 billion USD per annum worldwide are spent to repair and maintain concrete infrastructure alone [3]. Reinforced concrete (RC) is the most widely used material for construction in infrastructure industry which suffers corrosion related premature failures. Corrosion is a destructive electrochemical process that occurs between a metal and its environment [4]. The construction of concrete structures utilizes cement which is responsible for CO<sub>2</sub>

emissions leading to environmental pollution [5]. Hence, any effort in corrosion control strategies for improving the lifespan of concrete structures would lead to sustainable environment and persistent economy. Concrete is vulnerable to environmental degradation due to its inherent porous nature, because of which aggressive ions like chlorides penetrate into it which destroy the passive oxide layer on the steel/concrete interface, leading to corrosion. This, in turn leads to the formation of rust having 6 to 10 times more volume than parent steel volume, thereby generating additional tensile stresses inside the concrete, which lead to cracking and spalling of surrounding concrete [4,6-8].

It is not possible to eliminate altogether corrosion occurring in concrete but several corrosion control strategies which focus on either

\* Corresponding author.

E-mail address: [nsharma1\\_me17@thapar.edu](mailto:nsharma1_me17@thapar.edu) (N. Sharma).

<https://doi.org/10.1016/j.conbuildmat.2022.126495>

Received 14 October 2021; Received in revised form 11 December 2021; Accepted 14 January 2022

Available online 22 January 2022

0950-0618/© 2022 Elsevier Ltd. All rights reserved.

altering the corrosion mechanism or delaying the same have been reported. Researchers have reported to delay corrosion of reinforcing steel by reducing permeability of the concrete by introducing admixtures in concrete mix like fly ash, polymer fibers or healing microcapsules [9-14], or by applying coats or surface treatments on the concrete surface to make it impermeable [15-19], or by using corrosion inhibitors which prevent the entry of aggressive ions into the concrete [20-23]. Use of protective/sacrificial coatings on the reinforcing steel like galvanization, epoxy-based coatings, and zinc based cathodic protection etc. have been reported to be very effective for corrosion inhibition. The protective coatings delay initiation of corrosion by forming an impermeable and impenetrable layer on steel rebars. Sacrificial coatings, on the other hand, form a thin layer of a sacrificial metal like zinc, which has lower electrode potential than steel. Being more reactive than steel, zinc loses electrons in place of steel, thereby providing cathodic protection of steel rebars in concrete [24-28].

In recent years, epoxy-coated rebars (ECRs) have been considered to provide an effective and reliable method for mitigation of corrosion in aggressive media. It, however, needs further investigation for wider applications [29,30]. Epoxy coating layer provides an impermeable layer after complete curing of the film to act as a physical barrier to separate the steel substrate from the corrosive environment. The ECRs in RC structures compromise bond between steel and concrete but this problem can be tackled by modification in the development length for on-site application [31-33]. The biggest challenge in the use of epoxy coating on rebars is its brittle nature. It undergoes damage due to chemical and mechanical forces on site, due to which the long-term durability of these coatings can be compromised. Also, the presence of micro-pores in these coatings during fabrication leads to catastrophic failures with micro-pores acting as sites of corrosion/damage initiation. Studies have been reported for improving the long term durability of these epoxy coatings by modification using nano-fillers like nano clay, inorganic nano-particles like SiO<sub>2</sub>, TiO<sub>2</sub>, ZnO, and self-healing agents, etc. [5,34-46]. They have been reported to result in improved chemical resistance, better scratch and abrasion resistance and corrosion resistance of the epoxy coatings, and enhanced mechanical strength as compared to pure epoxy coatings. But they have their own limitations like complication involved in the synthesis procedure of some self-healing coatings, long term durability or organic nature.

In recent times, several studies have been reported for improving the corrosion protection of metals using graphene-based coatings. Graphene has attracted a lot of attention in the scientific research as well as in the industry because of its excellent properties like very high specific surface area, low density, excellent thermal and electrical conductivities high level of impermeability, hydrophobicity, chemical resistance and mechanical strength, which are desirable for a broad range of applications including semiconductors, battery energy, composites researches, etc. [47,48]. In a popular method for mass production of graphene (Hummer's method), graphite is used as the precursor material. Using strong oxidizing agents, it is chemically exfoliated to form graphene oxide, GO, which is converted to reduced graphene oxide (rGO) by chemical or thermal treatment [49]. Recently, Lee and Mahajan have presented a novel one-pot process for producing GO from coal, which can be then converted to rGO using the standard reduction techniques [50]. The process was shown to be environment-friendlier and less expensive. The rGO produced from both the methods is multilayered (MLG). Single layer graphene (SLG), on the other hand, is produced using a so-called bottom-up approach in which chemical vapor deposition is deployed for synthesis of graphene from carbon-containing chemical compounds such as hydrocarbons or silicon carbide.

Both SLG and rGO are reported to be hydrophobic with high water repellency. GO, on the other hand, is a polar and hydrophilic adsorbent due to large quantities of oxygen functional groups which having high water absorbing properties [51,52]. It has been reported that epoxy coatings can be modified with graphene and its derivatives to improve the ductility of coatings, enhance their corrosion inhibition capabilities

by making paths tortuous for large aggressive ions like chloride ions, and strengthen their barrier capability through high chemical inertness [53-65]. *Ghauri et al.* [59] studied and compared the anti-corrosion behavior of both GO and rGO in epoxy resin and demonstrated that a GO-based coating on mild steel is more promising due to the presence of the functional groups in GO sheets. *Liu et al.* [57] reported that GO-based modified epoxy coatings had lower current density in potentiodynamic polarization measurement, nearly twice in magnitude compared to pure epoxy coatings. Recently, *Zheng et al.* [53] reported that GO filler is excellent in bonding with epoxy matrix if it is used in optimum concentration; 0.3 wt% GO in epoxy resulted in superior performance. *Amrollahi et al.* [54] reported that GO sheets modified with polyaniline and incorporated in epoxy coatings give excellent anti-corrosion abilities. Graphene-based composites behave as cathodic corrosion inhibitors and effectively enhance the cathodic protection of coatings [56,66].

Owing to their unique properties of high specific surface area and good conductivity, both GO and rGO have proved themselves to be the best filler materials in industry [67-69]. GO is known to be more effectively dispersed as compared to rGO because when GO is dispersed in epoxy resin (before addition of hardener), the oxygen-functional groups on GO sheet surface will form bonds with epoxide groups of epoxy resin and improve its dispersion [70-73]. In addition, when GO and rGO incorporated into epoxy it enhances mechanical, thermal and electrical properties of epoxy composite [74,75]. *Wan et al.* [74] reported that silane functionalized GO improved the thermal and mechanical properties of epoxy composite. *Aradhana et al.* [75] reported that epoxy-GO adhesive system provides superior mechanical properties in comparison with epoxy-rGO adhesive system. But these nano-fillers encounter agglomeration during synthesis due to their high surface area. To minimize this problem as well as improve dispersion and bonding characteristics of graphene-based modified coatings, silane agents have been used during synthesis process [57,60,70-73]. *Liu et al.* [57] proposed the use of 3-aminopropyl-tri-ethoxy-silane (APS) and 3-Glycidialoxy Propyl Tri-methoxy Silane (GPTMS) as silane agents to functionalize graphene, whereas *Ramezanzadeh et al.* [73] proposed the use of Tetraethyl-orthosilicate (TEOS) and APS for silane modification. *Zheng et al.* [53] reported that low concentration of GO is preferable in eliminating agglomeration and promoting uniform dispersion; high concentration of GO leads to non-uniform coating surfaces. *Pourhashem et al.* [71] used 3-aminopropyl triethoxysilane (APTES) and GPTMS as silane agents to modify the surface of GO sheets. Improved adhesion of nanocomposite coatings was reported. *Aneja et al.* [70] reported APTES functionalized GO modified coatings for mild steel substrates and demonstrated that functionalization provides better barrier protection mechanism.

To further improve the mechanical behavior and toughness of epoxy coatings, multi-walled carbon nanotubes (CNTs) can also be used. *Yan et al.* [76] reported that CNTs incorporated in graphene displayed toughened structure of graphene through  $\pi$ - $\pi$  stacking domains and covalent bond. *Han et al.* [77] reported that addition of CNT very effectively reinforced epoxy adhesive and improve its mechanical properties by the formation of a rigid network of CNT in epoxy adhesive. *Gojny et al.* [78] reported that addition of CNT in epoxy nano-composites improve the material as well as the mechanical properties. Several studies have reported and concluded that CNTs noticeably enhance the properties of graphene by improving the dispersion and strength of nano-composites [68,76-80]. In this work, CNT has been used in epoxy coatings to improve which has been reported to help in dispersion of rGO and GO in epoxy and toughen the overall coating.

In this paper, we propose to investigate the corrosion inhibition capabilities of epoxy-based coatings nano-modified with GO and rGO along with CNTs. To the best of our knowledge, while several studies have been reported for corrosion protection of different metallic coatings using forms of graphene derivatives, no study has been reported so far for investigating the corrosion resistance capabilities of ECR reinforced concrete, nano-modified with different graphene derivatives.

**Table 1**  
Coating Details and Test Plan.

Coating No.	Nomenclature	Details	Samples		
			Plain bars	Bars in Concrete	Cylinders-Pull Out Testing
–	<b>Control</b>	Uncoated rebar	3	3	3
Coating 1	<b>PE</b>	Pure epoxy coating	3	3	3
Coating 2	<b>rGO/CNT</b>	Epoxy coating modified with rGO (0.4 wt%), CNT (0.1 wt%) and silane agents (0.5 wt %)	3	3	3
Coating 3	<b>GO/CNT</b>	Epoxy coating modified with GO (0.4 wt%), CNT (0.1 wt%) and silane agents (0.5 wt %)	3	3	3
Coating 4	<b>FrGO</b>	Functionalized rGO in silane solution without epoxy	3	3	3
Coating 5	<b>FrGO + GO/CNT</b>	Base layer of functionalized rGO without epoxy covered by epoxy coating modified with GO (0.4 wt%) and CNT (0.1 wt %). and silane agents (0.5 wt %)	3	3	3

There are many challenges vis-à-vis uniform dispersion of nano-materials, effect and efficiency of functional groups, actual performance of rGO & GO in epoxy coatings on rebars in concrete when they are subjected to alkaline concrete media, etc. which have been assessed and investigated in this research effort. The ECR nano-modified with graphene derivatives and CNTs were subjected to accelerated impressed current corrosion. The performance of these coatings was characterized using visual inspection, corrosion current and ultrasonic guided wave. Qualitative analysis of corrosion performance of prepared coatings was investigated by visual inspection periodically. Quantitative evaluation of corrosion inhibition capability was assessed by non-destructive and destructive testing. Corrosion current measurements and ultrasonic guided wave monitoring technique were used for non-destructive analysis whereas mass loss of corroded rebars and residual tensile strength of corroded rebars were used for destructive analysis. Further, prepared nano-modified graphene-based coatings were also tested for pull-out strength characteristics.

## 2. Experimental details

### 2.1. Materials used

GO and rGO used in this study were purchased from KNV's Incorporation (India), Multi-Walled Carbon Nanotubes (MWCNTs) were purchased from Reinste nano ventures Pvt. Ltd. (India). Tetra Ethyl Ortho-Silane (TEOS) and 3-Glycidialoxy Propyl Tri-methoxy Silane (GPTMS) used as silane agents were purchased from Sigma Aldrich Co. (India) and utilized without further purification. Acetic acid ( $C_2H_4O_2$ ) used as a pH modifier, ethanol ( $C_2H_5OH$ , 98%) as an initiator and distilled water were purchased from a local supplier. Two-part epoxy

having resin (Araldite CY 230-1) and curing agent (Aradur HY 951) was purchased from Excellence Resins Pvt. Ltd. (India). Plain mild steel bars of diameter 12 mm and length 300 mm were used in the present study and also purchased from a local supplier. All the materials for the preparation of coatings were used without any additional treatment.

In the present study, to further extend the scope in concrete structures undergoing corrosion, reinforced concrete samples were prepared with coated rebars. Ordinary Portland cement of grade 43 (IS: 8112-1989), and locally available fine and coarse aggregates (not greater than 10 mm) and tap water were used to prepare concrete mix. M20 grade concrete was prepared by concrete mix proportions of 1:1.45:2.91 (cement: sand: coarse aggregates) with water to cement ratio of 0.45. Average compressive strength at 7 and 28 days of prepared concrete was obtained as 18.1 N/mm<sup>2</sup> and 27.9 N/mm<sup>2</sup>, respectively. Concrete beams of size 100 mm × 100 mm × 250 mm were prepared with a centrally embedded single rebar of 12 mm diameter and length 300 mm (1 ft.) in the middle of the cross-section of the beam having projection of approximately 25 mm on both sides. The cast beams were removed from the mould after 36 h of casting and cured for 28 days at room temperature. After the curing period, these samples were subjected to accelerated impressed current corrosion (Section 2.3).

### 2.2. Test program & preparation of coatings

To examine the influence of graphene derivatives in epoxy coatings for investigating their corrosion inhibition performance in rebars, different coatings were prepared as outlined in Table 1. Basically, two types of graphene-based coatings were prepared— rGO based and GO based — to investigate their comparative performance with respect to corrosion protection in concrete structures. Additionally, functionalized rGO coat was prepared as per the methodology outlined by *Ahmadi et al. [72]*, and a dual arrangement of functionalized rGO and GO based coating was prepared.

Five different coatings were prepared along with one control (uncoated) sample bar. Coating 1 was pure epoxy coating, Coating 2 was epoxy coating modified with rGO/CNT and silane agents, Coating 3 was epoxy coating modified with GO/CNT and silane agents, Coating 4 was functionalized form of rGO without epoxy, and Coating 5 was an arrangement of FrGO with GO i.e. with a base layer of functionalized rGO layer covered by epoxy coat modified with GO/CNT and silane agents. The concentration of GO and rGO (0.4% by weight of epoxy) and CNT in the developed coatings have been used as an optimum level as recently suggested by researchers [54,68,80]. The uncoated as well as all the coated rebar samples were subjected to accelerated corrosion and examined using non-destructive and destructive analysis to evaluate their corrosion inhibition performances with and without surrounding concrete. Another set of coated rebars was also cast in concrete for pullout testing. All the samples were continuously monitored throughout the corrosion exposure period using ultrasonic guided waves and corrosion current, along with periodic visual inspection.

#### 2.2.1. Preparation of pure epoxy coating

For the preparation of this coating (PE), two-part epoxy resin and hardener were taken in the weight ratio of 10:1 and mixed by stirring using mechanical mixer at 500 rpm for 10 min. The resulting matrix was ready for coating. Plain mild steel rebars were cleaned using emery paper to remove rust present on rebars before coating. A rebar was coated with the epoxy matrix by a small paint brush and placed vertically for 6 h. This allowed the excess amount of material to flow by gravity and spread the coating evenly throughout the rebar section. The rebars were then cured in the oven at 80 °C for 3 days before subjecting them to accelerated corrosion or casting them in concrete. The dry thickness of the PE coatings was measured by standard electronic digital Vernier Caliper having a least count of 0.01 mm (10 μm). The average thickness of the pure epoxy coating was found to be 250 μm ± 40 μm.

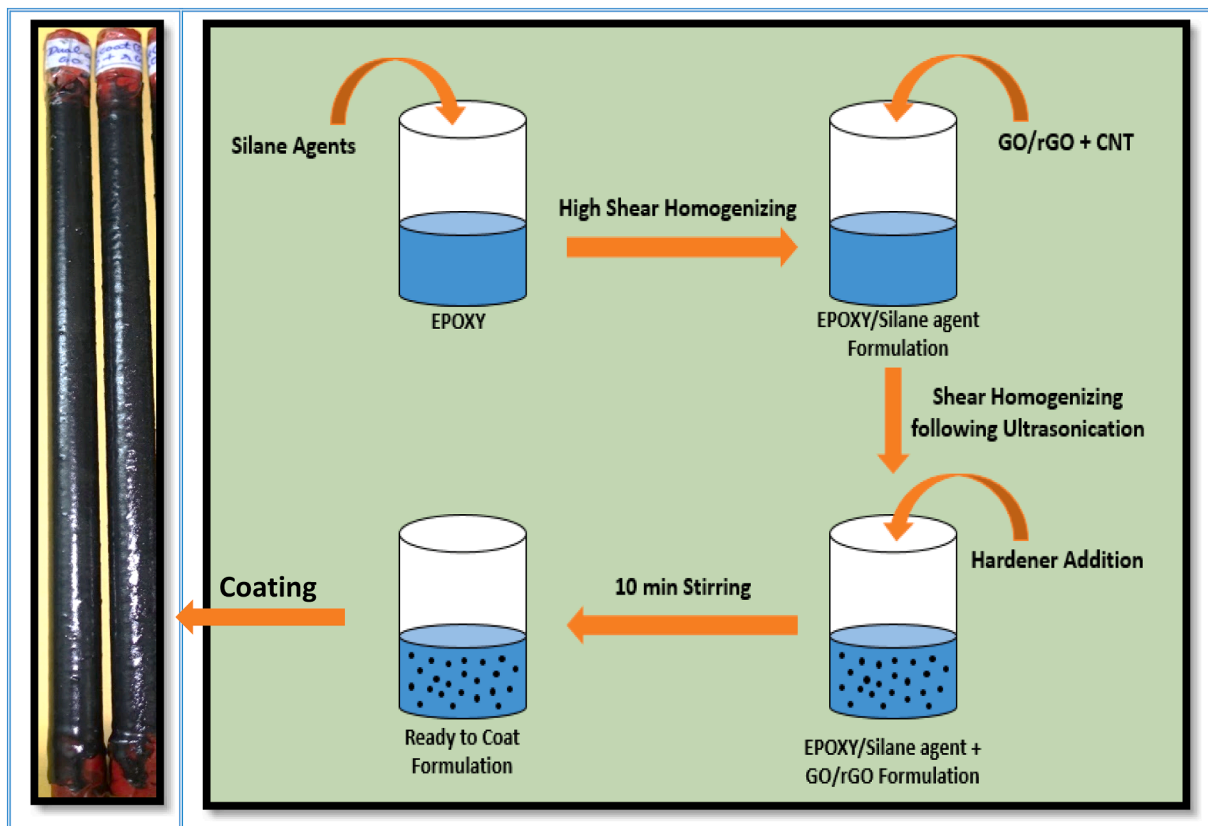


Fig. 1. Schematic diagram of synthesis of rGO/GO modified epoxy coating.

### 2.2.2. Preparation of graphene based modified coatings

Coating 2 (rGO/CNT) was prepared using conventional mixing method; its schematic diagram is shown in Fig. 1, which shows direct incorporation of silane agents and nano fillers in the epoxy resin. In 100 gm of epoxy resin, a mixture of 0.5 wt% of GPTMS and TEOS as silane agents by weight of epoxy resin were mixed using high shear homogenizer for 5 min to facilitate better dispersion of fillers and surface modification [57,73]. To this mixture, rGO by 0.4 wt% and CNTs by 0.1 wt% of epoxy resin were incorporated to enhance the barrier properties and strength of coating matrix, respectively. CNTs are also recommended for reinforcing composite structure and improvement in

dispersion of rGO [68,76-80]. Both rGO and CNTs were mixed in the resin and subjected to shear homogenizing at 20,000 rpm for 10 min, and further subjected to ultrasonication using a probe sonicator for 10 min. During ultrasonication, an ice bath was used to control the temperature of the matrix. Post-ultrasonication, the matrix solution was cooled for 10 min to reduce its temperature, following which the sample was subjected to constant stirring at 500 rpm using a mechanical stirrer, with the hardener (10:1) added gradually to the coating matrix for 5–10 min. The matrix was then coated on the plain bars with paint brush. For curing, the procedure described above for curing Coating 1 was deployed. The average dry thickness of the rGO/CNT modified epoxy coatings was measured as  $270 \mu\text{m} \pm 40 \mu\text{m}$ .

For the preparation of Coating 3 (GO/CNT), its application and curing, the procedure identical to that described above was followed by replacing GO (0.4 wt% by epoxy resin) in place of rGO. The average dry thickness of the GO/CNT modified epoxy coatings were measured as  $270 \mu\text{m} \pm 40 \mu\text{m}$ .

Owing to the hydrophobic nature of rGO which can improve the corrosion resistance by repelling water and other aggressive ions, another rGO coating was prepared by its functionalization. Coating 4 (FrGO) was prepared by the procedure mentioned by Ahmadi et al. [72] for silanized graphene oxide nano-sheets, as follows.

Two solutions were prepared, solution A and solution B. In solution A, functionalized rGO was prepared by mixing 46.92gm of ethanol, 0.575gm of distilled water and 2.5gm of GPTMS using constant magnetic stirring for 10 min at room temperature. In the resulting solution, rGO was added at a concentration level of 2.5 gm/l. The pH of the mixture was adjusted to 4.5 using acetic acid and stirrer using magnetic stirrer for 2 h. The pH was then increased to 11 using NaOH solution and stirrer for 1 h for condensation reaction. It was then subjected to ultrasonication using a probe sonicator for 10 min followed by washing using mixture of deionized water and ethanol (60:40 w/w). The washed functionalized rGO was extracted from the solution using vacuum



Fig. 2. Control bar and prepared coated bars.

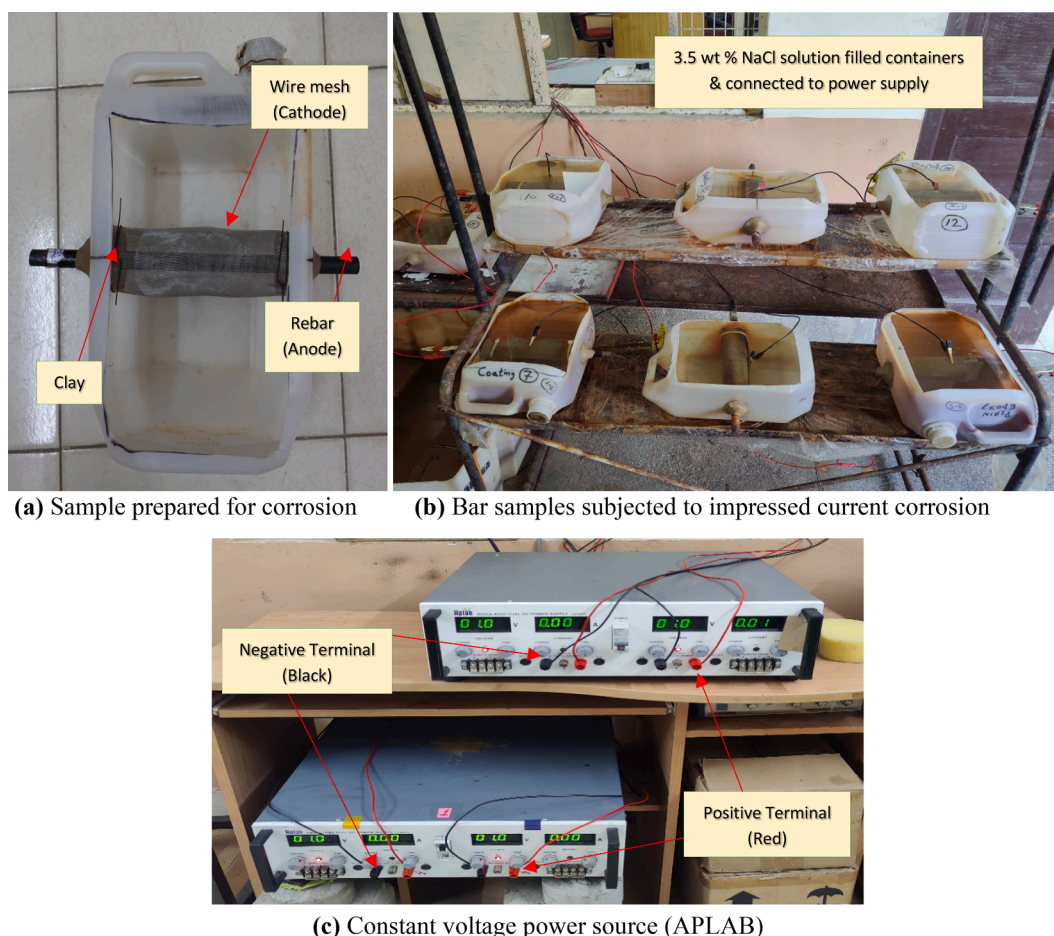


Fig. 3. Set-up for corrosion testing.

filtration. Simultaneously, silane solution was prepared (solution B), by mixing 40gm ethanol, 0.78gm GPTMS, 1.72gm TEOS and 7.5gm distilled water using magnetic stirring. Functionalized rGO extracted from solution A was added into solution B, accompanied by continuous magnetic stirring for 1 h followed by ultrasonication for 10 min. Plain steel rebars were coated with the prepared solution using air spray having pressure of 2 atm. After application of the first layer of solution the rebar was dried in the oven at 120 °C for 10 min. This coating and drying process was repeated 3 times to facilitate ensure uniform distribution of rGO throughout the rebar section. After 3rd layer of coating application, samples were dried at 120 °C for 30 min. The average dry thickness of FrGO coatings was  $70 \mu\text{m} \pm 10 \mu\text{m}$ .

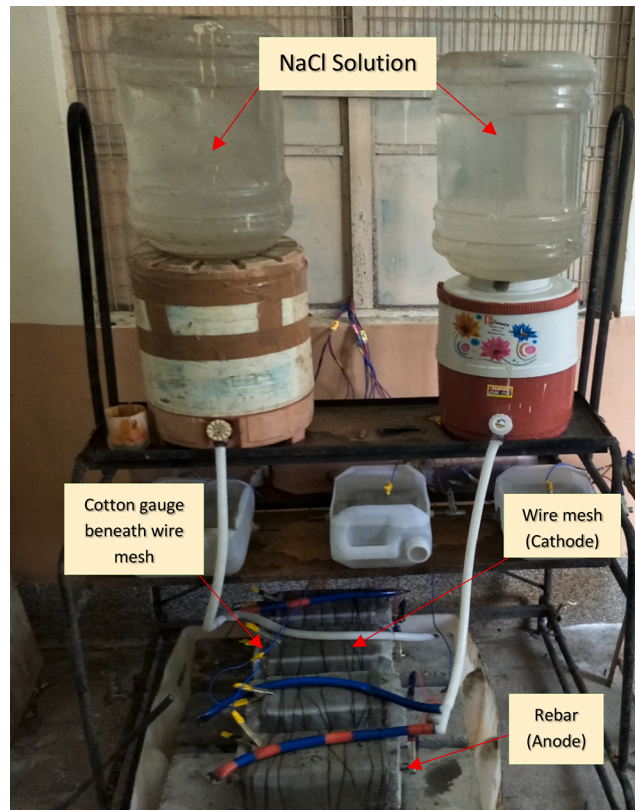
Coating 5 (FrGO + GO/CNT) was prepared using a base coat of FrGO and applied to rebar samples, which were dried and further coated with formulation described for Coating 3 (Table 1) and cured. The average dry thickness of FrGO + GO/CNT coatings was  $310 \mu\text{m} \pm 50 \mu\text{m}$ .

All the prepared samples prepared are shown in Fig. 2. It can be noticed that pure epoxy has transparent glossy coat whereas rGO/CNT and GO/CNT modified epoxy coat look pure black. The FrGO coatings were hardly noticeable and FrGO + GO/CNT coatings had a rough top surface, mostly due to the base coat of FrGO which creates an uneven layer on the rebar samples. Three samples of each of the coated rebars were prepared for testing in air as well as for embedding in concrete and additionally 3 samples of each coating were prepared for casting in concrete cylinders for pull out testing (Table 1).

### 2.3. Accelerated impressed current corrosion

All the steel bar samples, plain as well as embedded in concrete, were subjected to accelerated impressed current corrosion at constant voltage of 1 V and 15 V, respectively (Fig. 3). High voltage is used for impressing corrosion in coated bars in concrete to accelerate corrosion in a lesser duration of time to arrive at useful strategies for corrosion inhibition and protection [35,81-86,91-93]. A brief description of the testing follows. For plain rebar samples, a container of width less than 1ft. with holes at the sides to place the rebar was prepared. The rebar was placed in the middle of the container with projection of 20–25 mm on both sides, and its ends were sealed with clay to minimize corrosion at the junction. A stainless steel wire mesh was wrapped around rebars to act as a cathode in the corrosion cycle (Fig. 3a) and was connected to the negative terminal of the constant voltage power supply (APLAB Make, Rating of 0-5A, 0-64 V). The rebar served as anode and was connected to positive terminal of the power supply. The container was then filled with the 3.5% NaCl solution. Plain rebar samples were corroded at constant voltage of 1 V throughout the testing period. Corrosion current was noted after every 6 h of interval to quantify corrosion as non-destructive evaluation for all the rebar samples without concrete. Three samples of each rebar coating type were tested to ensure uniformity and repeatability of results.

Similarly, for rebar samples embedded in concrete, the concrete specimens were wrapped with cotton gauge for maintaining uniform moisture by brine solution drip and a stainless steel wire mesh was wrapped on top of it (Fig. 3d). The bars acting as anode and stainless steel wire mesh as cathode were connected to the power supply and



(d) Concrete samples subjected to accelerated corrosion

Fig. 3. (continued).

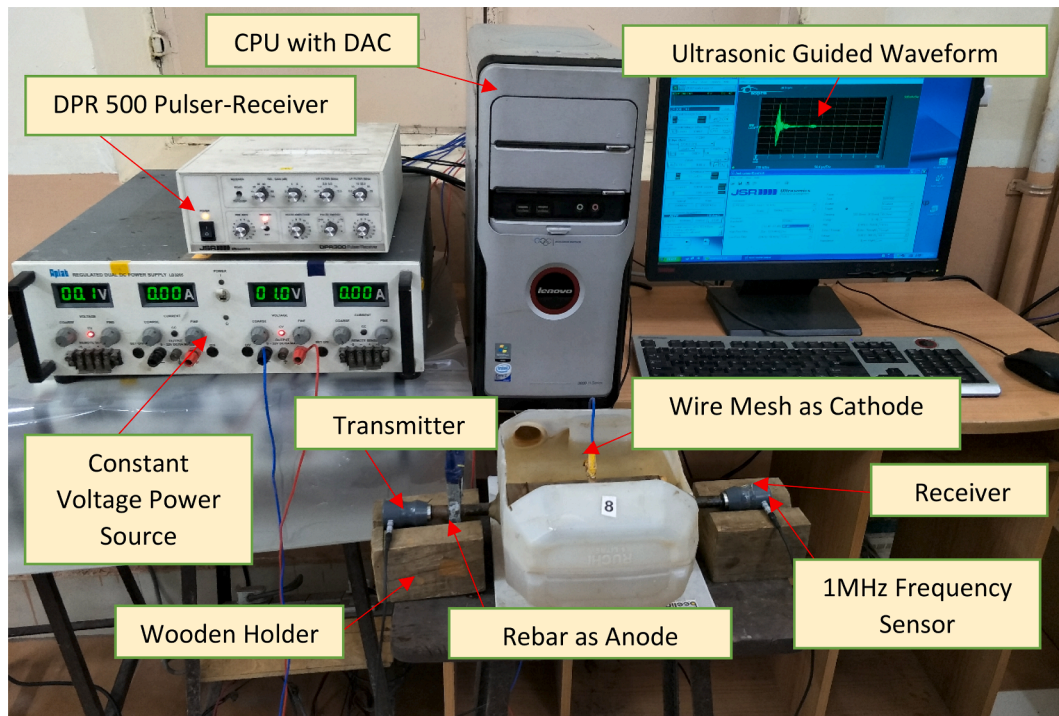
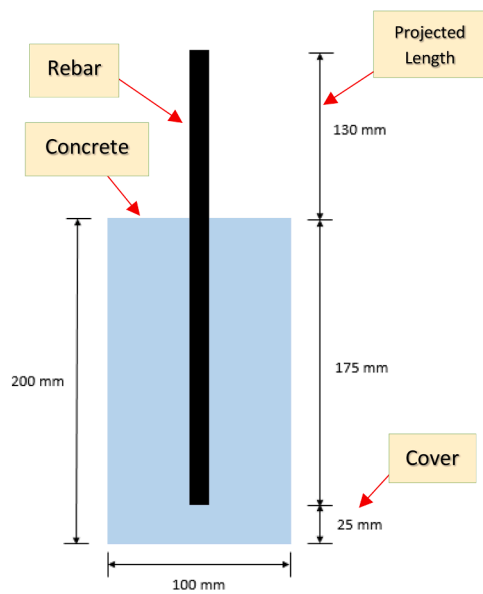


Fig. 4. Setup for ultrasonic guided wave monitoring.

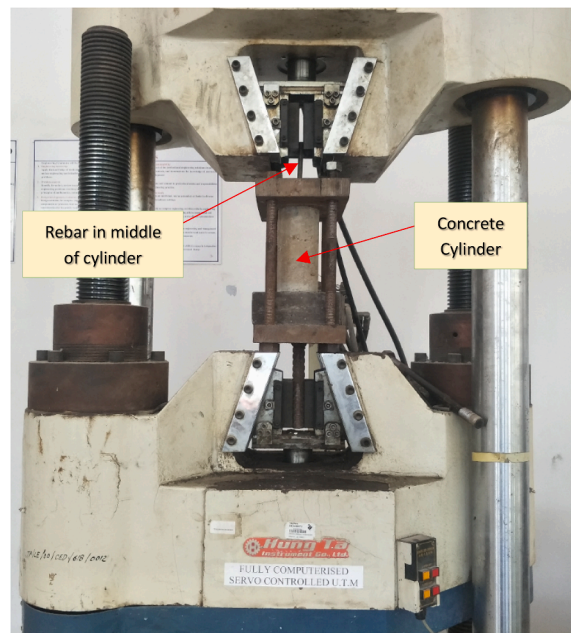
accelerated corroded at constant 15 V voltage. Corrosion current was noted after every 12 h interval to quantify corrosion for all the rebar samples embedded in concrete. Three samples with each type of rebar

embedded in concrete were tested and evaluated.

It is important to know that addition of conductive rGO, GO and CNT may increase the electrical conductivity if the concentration of nano-



(a) Schematic of specimen



(b) Pullout testing in UTM

Fig. 5. Pullout test specimen and Set-Up.

filler exceeds the percolation threshold limit. In this study, the concentration of these three moieties used is less than the percolation threshold limit [87-90], so an excellent corrosion protection has achieved without forming an electrochemical circuit in the system chosen. To further substantiate this hypothesis, a simple test of measuring conductivity sound check was done for all the coated rebars using multi-meter (Model- Rishabh, 400A AC-DC). It was found that no sound was produced by multi-meter for all coatings indicating coating surface is non-conductive in nature.

#### 2.4. Ultrasonic guided wave monitoring

The effectiveness of corrosion inhibition of different types of coatings mentioned in Table 1 was also studied using non-destructive technique of ultrasonic guided waves propagated through rebars. The process of monitoring was similar to that suggested by Sharma et al. [35,91]. The conventional ultrasonic guided wave mode of L (0, 7) was used for excitation at 1 MHz high frequency guided wave, which was reported to be effective in picking up pitting effect of corrosion in 12 mm rebars [35,82-85,91-93]. A conventional UT system consisting of pulser-receiver device (DPR 500, Karl Deutsch Make), 12 mm diameter cylindrical transducers (Karl Deutsch Make) with frequency of 1 MHz and Data Acquisition Card (DAC) of Aquiris Make was used for ultrasonic testing. The ultrasonic testing was done in through-transmission mode in which the transmitter as well as receiver probes were kept along the longitudinal axis of the rebars (Fig. 4).

The transmitter and receiver transducers were kept in place using a holder assembly to maintain constant pressure at both ends of the rebar throughout the testing process. Briefly, the UT system excites the transmitter which sends guided wave signals in the rebar, with the receiver receiving the transmitted waves at the other end. The transmitted signals through the corroding rebars are then analyzed to assess the level of deterioration. It is marked by fall in transmitted signal strength due to the pitting and area reduction in the rebars undergoing accelerated impressed current corrosion leading to signal attenuation. Multiple reflections and guided wave mode scattering due to pits in rebars cause drop in signal strength. Fall in signal vis-à-vis signal in the initial healthy bar indicates deterioration in the rebars due to corrosion.

In our experiments, variation in the strength of transmitted signal represented in the form of peak to peak voltage ratio (w.r.t. amplitude of the healthy bar) with increasing corrosion was measured. It is important to note that while taking ultrasonic readings, the power supply was kept switched off to avoid any interference of signals.

#### 2.5. Destructive testing

##### 2.5.1. Mass loss and residual tensile strength

After the rebars were subjected to designated levels of deterioration, they were subjected to destruction testing to estimate their residual strength. To this end, mass loss and residual tensile strength of steel were evaluated to correlate the non-destructive testing results and quantify the extent of corrosion. The corroded samples were removed from the container or extracted from the concrete and then cleaned with an iron brush to remove the rust product and washed with acetone to remove all the remaining corrosion products present on the rebars. Cleaned and dried rebars were then weighed to evaluate the mass loss in rebars due to corrosion. After weighing the rebars, they were tested on Universal Testing Machine (Hung Ta Make, Capacity 1000 KN) at the load rate of 0.5 kN/second to determine their residual tensile strength.

##### 2.5.2. Pullout strength testing

Another set of coated rebars were cast in concrete and subjected to pullout test to evaluate the effect of epoxy-based coatings on the bond strength between concrete and the rebar. Any kind of coating on rebars in concrete should not compromise its bond strength with surrounding concrete. This is the basis of design of reinforced concrete sections and hence, it is very important to investigate the bond effect of coatings on rebars. All five differently coated rebars coatings and control rebars were cast in concrete cylinder of 100 mm diameter and 200 mm length. The concrete design mix used for the preparation of cylinders was similar to that mentioned in Section 2.1. Cylinder specimens having 12 mm mild steel rebars in the middle of the cross-section were placed at a cover of 25 mm from the bottom and projected at the other end by 130 mm out of the cylinder (Fig. 5a). The casted cylinders were cured for 28 days at room temperature and then subjected to pull-out strength testing using Universal Testing Machine (Hung Ta Make, Capacity 1000 KN) at

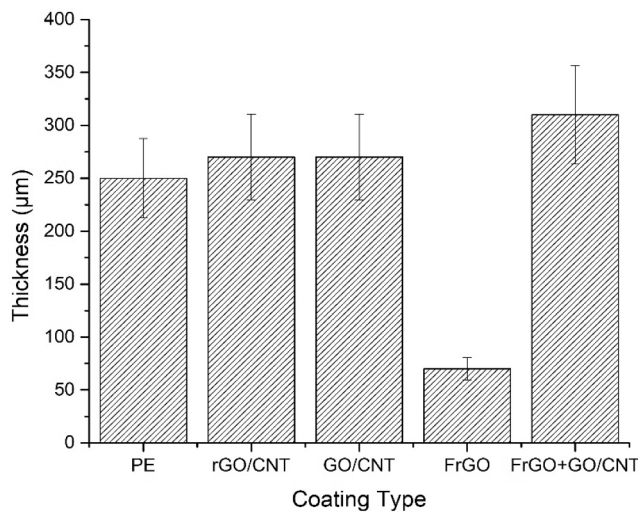


Fig. 6. Average thickness of different types of coatings.

a loading rate of 0.5 kN/second till failure (Fig. 5b). Three samples of each type of the coated rebars were tested to calculate the average pullout strength.

### 3. Results and discussions

#### 3.1. Coating thickness analysis

For each type of coating (Coating 1-Coating 5, Table 1), thickness of a total of 10 samples for each coating type was measured using a digital Vernier caliper (Zhart Make, least count of 10 μm). For each of the samples, thickness of the coating was measured at three different

locations 25 mm from top, 25 mm from bottom and at middle of the rebar. The average thickness of each of the five coatings is plotted in Fig. 6.

Since the rebars were the plain mild steel rebars without ribs, rebar thickness was almost constant throughout the section, with little deviation (maximum of 50 μm in some rebars). Based on the 10 measurements at 3 different spots, it was concluded that the average thickness of the PE is about 250 μm with standard deviation of 40 μm. On the other hand, the rGO and GO coatings had average thickness of 270 μm with standard deviation of 40 μm. The FrGO coating was about 70 μm thick with deviation of 10 μm, and the thickness of FrGO + GO coatings was measured to be 310 μm with standard deviation of 50 μm.

#### 3.2. Visual observations

##### 3.2.1. Coated rebars

All the coated rebars were subjected to accelerated impressed current corrosion and their performance was assessed by visual observations and through variation in corrosion current and ultrasonic guided wave measurements. Samples were periodically removed from the power supply and observed visually to examine the effect of accelerated corrosion. Accelerated corrosion was stopped when the guided wave signal vanished completely. In **control rebars** with no coating, corrosion initiated within the first hour of the exposure and the bar experienced uniform corrosion throughout the length. After 7 days of accelerated corrosion exposure, the rebars suffered pitting at different locations and within 8–9 days of exposure, ultrasonic guided wave signals completely vanished and accelerated corrosion testing was stopped (Fig. 7).

For the **PE coated rebars**, within 5–10 days of accelerated corrosion, delamination of the epoxy coatings from rebars was observed by bubble formation at different spots beneath the epoxy coatings (Fig. 8). It indicates penetration of aggressive chloride ions into the epoxy matrix by breakdown of passive layer indicating initiation of corrosion. After 15



Fig. 7. Visual images of control (uncoated) rebars.

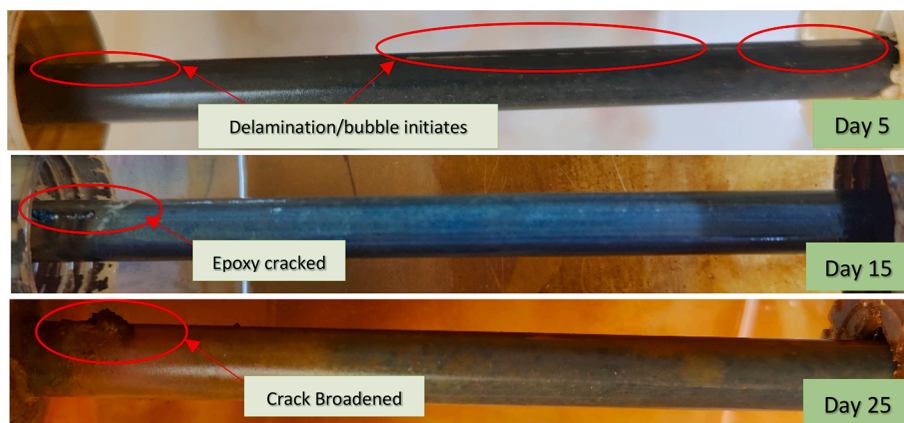


Fig. 8. Visual images of PE coated rebars.



Fig. 9. Visual images of rGO/CNT coated rebar.

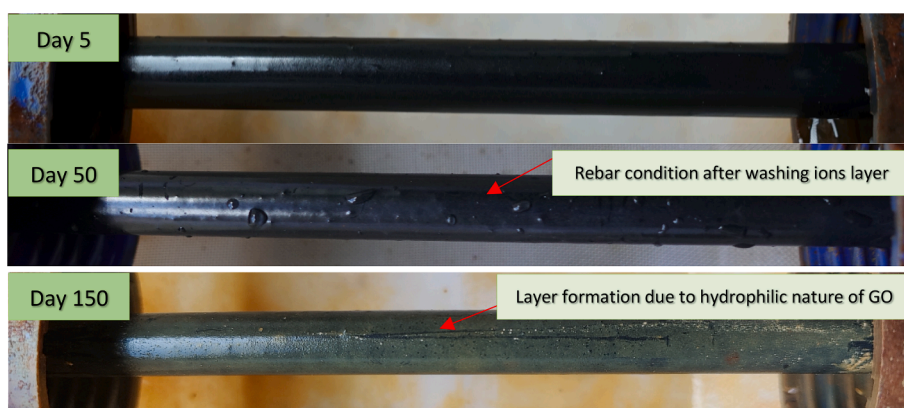


Fig. 10. Visual images of GO/CNT coated rebars.

days, it was observed that at one typical location of a PE bar, epoxy layer cracked leading to further ingress of aggressive ions and deterioration. After 25 days, this crack broadened and accumulation of corrosion product was noticed near it, indicating localized pitting of the rebar at this spot. With increasing corrosion exposure, widespread cracking was observed accompanied by widespread pitting, which led to drop in ultrasonic guided wave signal, with the signal vanishing completely in 44 days as against 8–9 days in the uncoated rebar. Similar observations were made in other similar PE coated rebar samples.

The *rGO/CNT coated rebars* held off corrosion for significant duration as compared to the PE coatings; no delamination or bubble formation was observed for 30 days (Fig. 9), possibly due to the hydrophobicity and tortuous path provided by the rGO nano particles in the epoxy matrix. The existence of CNTs toughens the graphene structure and improves the mechanical strength of epoxy nanocomposite [68,76,77]. After 30 days, initiation of corrosion was observed by breakdown of the passive layer, and within 40 days corrosion spots or bubbles were clearly visible, indicating accumulation of the rust product. The corrosion spots lead to formation of corrosion crack in about 60 days. In 100 days, the localized corrosion pit widened due to continuous pitting at that location. Spot widened but it is important to note that pitting was not widespread at many locations as in the control or PE coated bars, but once it initiated at a point, it could not be arrested. This was confirmed by a continuous drop in the ultrasonic guided wave voltage amplitude, which vanished in 125 days (average for all samples). Compared to 8–9 days for the control bar and 44 days for the pure epoxy coated bar, rGO/CNT coated bars perform significantly better in preventing corrosion.

Impressive as this result was, our data indicated that *GO/CNT*

*coated rebars* perform even better than the rGO/CNT coated rebars. There was no delamination or failure noticed in the form of local pits or cracks in the coating. After 60 days of accelerated corrosion, the rebar looked as healthy as on day 1 (Fig. 10). Even after 125 days of accelerated corrosion, the GO/CNT coated rebar showed no visible sign of deterioration in the form of pits or failure of coating or cracking at any point. This observation was consistent in two samples out of three. Only 1 sample showed some reddish brown stain at a localized point but no other visible increase in corrosion current or drop in guided wave signals was observed in this rebar. Till 150 days of accelerated corrosion of GO/CNT coated rebars, no change in non-destructive testing parameters of corrosion current as well as ultrasonic guided wave signals was observed in all the three samples.

The superior performance of GO/CNT modified epoxy coatings on rebars is due to large specific surface area provided by GO and presence of oxygen-functional groups on GO sheet surface which provides a dense impermeable layer uniformly distributed in the brittle epoxy, which, in turn, provides a tortuous path and entraps the entry of aggressive chloride ions [59]. Also GO dispersed more effectively than rGO in epoxy because GO oxygen functional groups form bonds with the epoxide groups of epoxy resin and improve its dispersion [70–73]. Also, optimum percentage of GO (0.3–0.4 wt%) in epoxy matrix eliminates the minor coating defects since GO gathers around the defects in coating and eliminates them and provides impermeable coating [53,55]. Furthermore, even though GO is hydrophilic but in the investigated concentration level of 0.4% by weight of hydrophobic epoxy, GO exhibits overall hydrophobicity, which might be the reason for this type of performance of GO modified coated rebars [53]. Another reason for their outstanding performance can be the lower conductivity of GO,

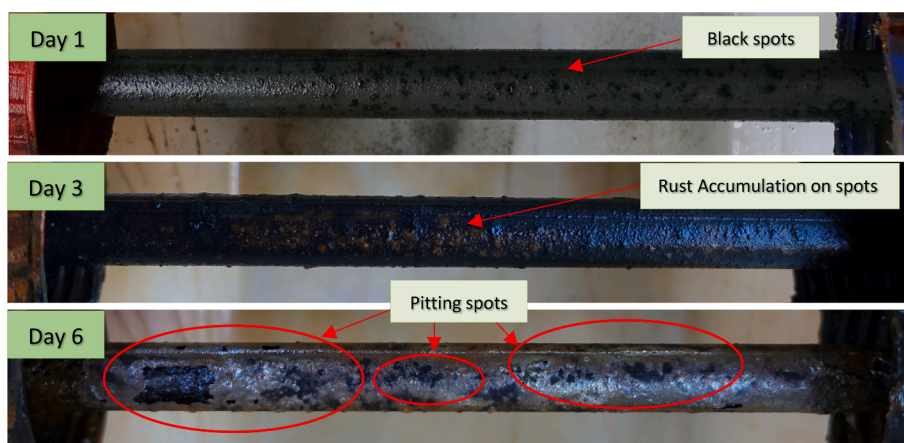


Fig. 11. Visual images of FrGO coated rebars.

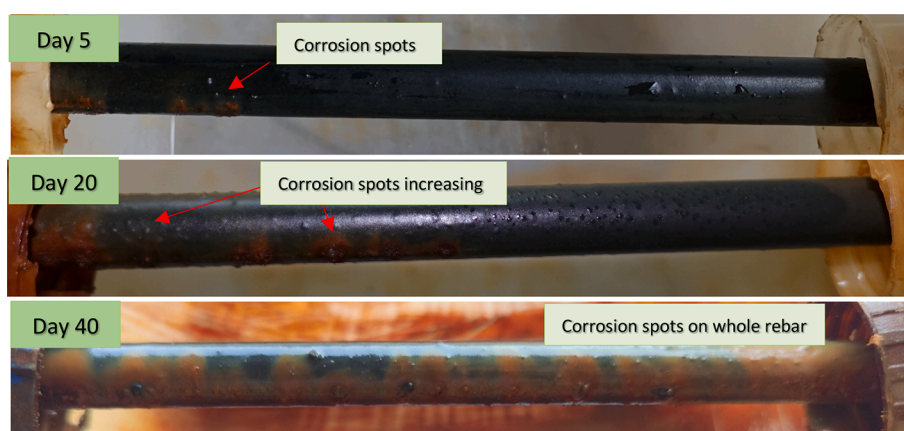


Fig. 12. Visual images of FrGO + GO coated rebars.

which is reported to be approximately 10 S/cm for GO in comparison with 0.01 S/cm for rGO [56]. It has been reported that lower electrical conductivity of epoxy-GO adhesive is due to presence of oxygen functional groups in GO in comparison to epoxy-rGO adhesive which has reduced functional groups, which may assist in delaying the corrosion process [75]. Also, the presence of CNT along with GO in epoxy adds to the mechanical strength and toughness of these coatings [76,77].

A significant observation during testing is the presence of salt deposits on GO coated rebars. This can be explained by the hydrophilic nature of GO which attracts saltwater but the epoxy admixed with GO and CNT forms a dense impermeable network or layer which does not allow the entry of these chloride ions into the coating; they accumulate on the rebar with no penetration inside. The salt deposits are easily rubbed off by hand and the GO/CNT coated bars appear as originally coated shiny bars. The coating remained intact even after 150 days of accelerated corrosion.

In functionalized coated rebars without epoxy (*FrGO coated rebars*), corrosion initiated in similar pattern as in the uncoated rebars and performed worse than rGO/CNT coated rebars since there was no epoxy present in the coating that could make it more vulnerable to the penetration of aggressive ions. Within 2–3 h of exposure, corrosion was initiated and after one day of corrosion, black spots were noticed on the rebars. Accumulation of the rust product was observed in 3 days, indicating pitting or progression of corrosion (Fig. 11). Within 7 days of accelerated corrosion, the rebar was badly corroded and the corrosion pits were observed at various locations. The guided wave signal vanished in 7 days earlier than for even the uncoated rebars. Similar results were noticed for all the other similar samples indicating more aggressive

corrosion than control samples. This can be explained by the fact that the highly conductive nature of rGO results in acceleration of the corrosion by speeding up the cathodic reaction by up-take of electrons at a higher rate [57,60,63,76]. The clear indication is that although rGO is hydrophobic and functionalized with GPTMS, without epoxy this layer is ineffective and its conductive nature overpowers its hydrophobicity.

For the last coating considered on this study *FrGO + GO/CNT coated rebars*, distinctive features were observed as compared to the other epoxy coated rebars. During accelerated corrosion testing within first week of exposure, several corrosion spots were observed on the rebars in 5–7 days (in all three similar samples) (Fig. 12). This is probably due to the base layer of FrGO without epoxy which becomes the weak link and initiates corrosion. The aggressive chloride ions easily break this layer since there is no epoxy. Also, the conductive nature of rGO nano particles in this layer further accelerates the cathodic reaction which overpower its hydrophobic property. Within 40–50 days, the corrosion spots spread on the entire rebar with accumulation of the rust product, which finally leads to corrosion cracks during the later stages. The FrGO + GO/CNT sample could withstand accelerated corrosion for an average of 110 days (average of 3 samples). The presence of GO/CNT in the top layer with epoxy helps impermeable layer to hold corrosion exposure for significant duration.

The performance of the FrGO + GO/CNT coating is somewhat better than the FrGO coating, due to the resistance offered by the top coating of GO/CNT with epoxy to corrosion progression though it initiates in the underlying FrGO layer having no epoxy. For the FrGO + GO/CNT coating, it can be concluded that the immediate layer or base layer on the rebar should be very strong so that corrosion does not initiate. The

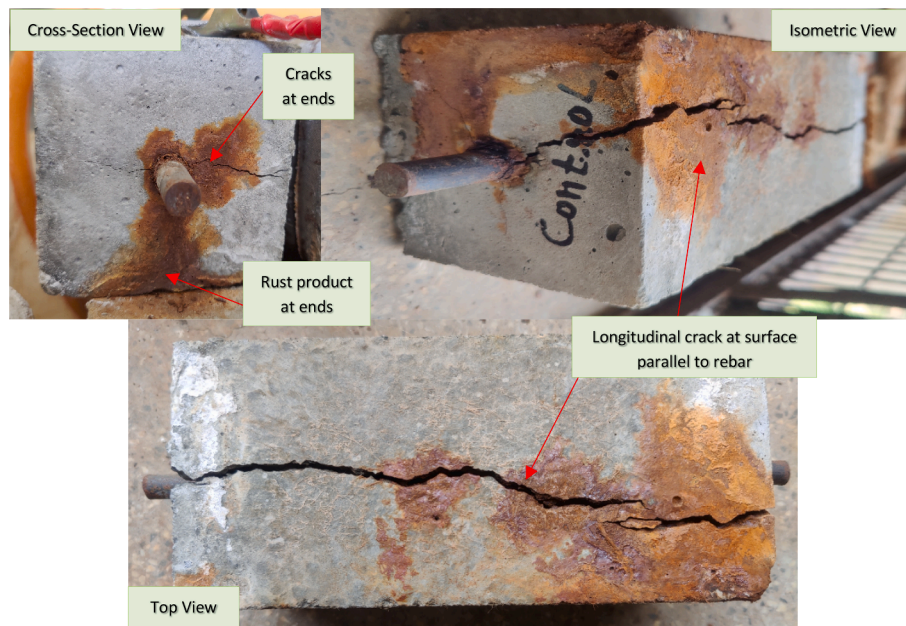


Fig. 13. Visual images of beam reinforced with uncoated bar undergoing accelerated corrosion.

top coating of GO/CNT with epoxy could not hold the corrosion progression for longer duration as observed in rebars coated with only GO/CNT since corrosion had already spread and initiated in the FrGO layer. An important conclusion is that FrGO without epoxy is ineffective, even if used in combination of GO/CNT with epoxy as top layer.

### 3.2.2. Coated rebars embedded in concrete

During accelerated corrosion of the coated rebars embedded in concrete, visually three stages were observed. In the first stage, the rust product accumulates near the projected end of concrete section indicating initiation of corrosion. With the progression in corrosion, a crack appears on concrete cross-sectional ends. In the final stage, longitudinal cracks originate from sectional ends, which separate the concrete section into pieces. For the **control rebar** concrete specimens, the rust product was observed within 7–10 days of accelerated corrosion from the projected end of bar from concrete, and cracks appeared at the cross section ends within 15–16 days (Fig. 13). The side cracks progressed further in the form of surface longitudinal crack parallel to reinforcing bar (Fig. 13) in 25–29 days, which divided the concrete section into pieces. The control concrete specimen at that stage was in a highly dilapidated condition.

The coated reinforced concrete specimens were accelerated corroded for 90 days. In the **PE coated rebar** reinforced concrete specimen, the rust product from sides appeared after 25–35 days in comparison to 7–10 days in the control specimen. Cracks started appearing at the ends within 70 days of corrosion, but these cracks were not as wide as those observed in the control specimen after 90 days of accelerated corrosion of PE specimens; only hair line cracks were observed on the surface of concrete.

For the **rGO/CNT coated rebar** concrete specimens, the rust product accumulation appeared within 50–60 days of accelerated corrosion and no cracks were observed either at the sides or on the surface in 90 days. However, in the **GO/CNT coated rebar** concrete specimens no corrosion product was observed at the ends and no visible cracks appeared in concrete even after 90 days of accelerated corrosion.

The **FrGO coated rebar** concrete specimens perform analogously to the concrete samples with control rebar; within 10 days of accelerated corrosion rust products accumulated near the ends and after 30 days of exposure longitudinal crack on the surface was observed leading to concrete specimen in a dilapidated condition. In the **FrGO + GO/CNT**

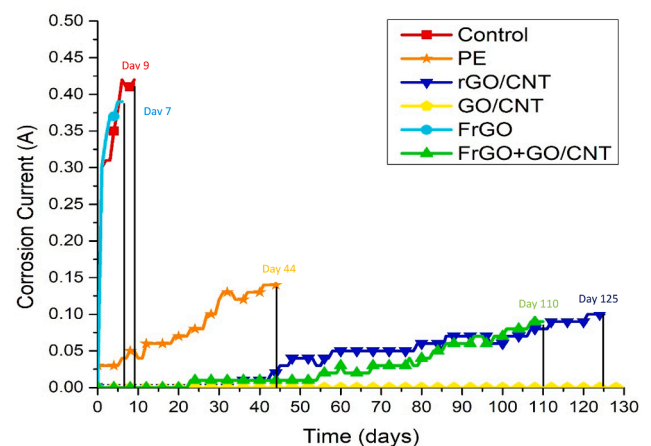


Fig. 14. Variation in corrosion current of rebars.

**coated rebar** concrete samples, within 45–50 days, the rust product accumulation was observed near the ends, and after 90 days of accelerated corrosion hair line crack was observed at the ends but no crack was observed on the longitudinal surface.

### 3.3. Corrosion current

#### 3.3.1. Coated rebars

During accelerated corrosion testing of the rebars only, a constant voltage of 1 V was applied to the sample to accelerate the corrosion process. The corresponding variation in the corrosion current was monitored regularly and is represented in Fig. 14. Increase in corrosion current is an indication of corrosion initiation and progression. Further, sudden jump in corrosion current indicates that the coating gives way and aggressive ions penetrate and break the passive layer of oxides on the bars. In the samples with **control rebars**, this jump was observed within 2–3 h of accelerated corrosion exposure and corrosion current suddenly jumped from 0A to 0.3A. Further, the corrosion current kept on increasing at a constant rate and reached to a value of 0.42A in 9 days, at which time the ultrasonic guided wave signal completely vanished

followed by removal of the sample.

In the **PE coated rebar**, small corrosion current was observed initially at the start of testing between 0.01A and 0.03A which remained constant till 6–7 days. After 6 days, sudden increment in corrosion current was observed indicating initiation of corrosion by breakdown of the passive layer as confirmed visually by the formation of bubbles indicating delamination of coating after 5 days. Pure epoxy was thus successful in delaying the initiation of corrosion up-to 6–7 days as against 2–3 h in control bars. Also, the rate of progression of corrosion in the PE coated rebars is very low as compared to control rebars. When the corrosion spots got converted into large cracks, a steep jump in the corrosion current between 29th –34th day was noticed. Overall, the PE coated rebar sustained corrosion up to 44 days with a corrosion current of 0.14A as compared to 9 days and 0.42A in the control bar, respectively.

In the **rGO/CNT coated rebars**, first increment in the corrosion current was noticed after 36–40 days of accelerated corrosion indicating breakdown of passive layer and corrosion initiation as against 6–7 days for the PE coated bars. This indicates substantial improvement in epoxy coating after admixing it with rGO and CNTs as against pure epoxy. Further progression of corrosion in rGO/CNT was slow with very small increase in corrosion of 0.05A in 75 days; the corrosion current reached a maximum value of 0.1A in 125 days of accelerated corrosion. This improvement can be attributed to a dense, impenetrable network formed in the epoxy which blocks entry of aggressive ions to the rebar. Also, since rGO is hydrophobic it repels the saline solution and improves its corrosion barrier resistance as compared to the PE coating.

As already discussed, in the **GO/CNT coated rebars** no increase or change in corrosion current was noticed even after 150 days of accelerated corrosion, indicating there is no initiation of corrosion during the entire corrosion exposure period. It was also confirmed by the visual observations in GO/CNT coated rebars, which showed no sign of degradation or deterioration even after 150 days of exposure. Out of the three samples tested with GO/CNT modified coatings, one of the sample showed reddish brown stains after 150 days of accelerated corrosion but there was no visible rise in the corrosion current. Dense and impenetrable network of GO with CNT in epoxy coating on rebar is even more effective than the rGO/CNT network. It can be concluded that GO modified coatings can effectively delay corrosion initiation for much larger durations with superior performance.

The **FrGO coated rebars** behaved almost similar to the control rebar. Within 2–3 h of corrosion exposure, corrosion current reached to 0.3A – 0.34A indicating the breakdown of passive layer and initiation of corrosion. But an important difference between the two is that the FrGO coated rebars did not corrode uniformly throughout as the control rebar. Several pits throughout the length resulting in localized corrosion were observed compared to uniform corrosion in control rebars. This confirms our earlier conclusion that FrGO without epoxy is not effective at all and the rebar will behave similar to the uncoated rebar. Corrosion current reached maximum of 0.38A-0.39A after 6 days of accelerated corrosion and ultrasonic signal vanished after 6–7 days (average of all three samples).

In the **FrGO + GO/CNT coated rebars** with FrGO at base layer and GO/CNT as top layer corrosion spots were observed visually within 7 days after having been subjected to accelerated corrosion, but first increment in corrosion current was noticed only after 22 days, indicating breakdown of passive layer and initiation of corrosion. The reason for the visual corrosion spots not accompanied by any change in corrosion current is probably due to their being localized and small size rather than deep pits which induce current change. Initially, the progression of corrosion was very slow as compared to the rGO/CNT coated rebars, but it accelerated after 70–80 days of exposure and reached to almost the same level as for the rGO/CNT coated rebars at the end of testing. The current in this dual coated bar reached 0.1A in 110 days and their ultrasonic guided wave signals completely vanished in 110 days of exposure. Acceleration in later stages is probably due to weaker

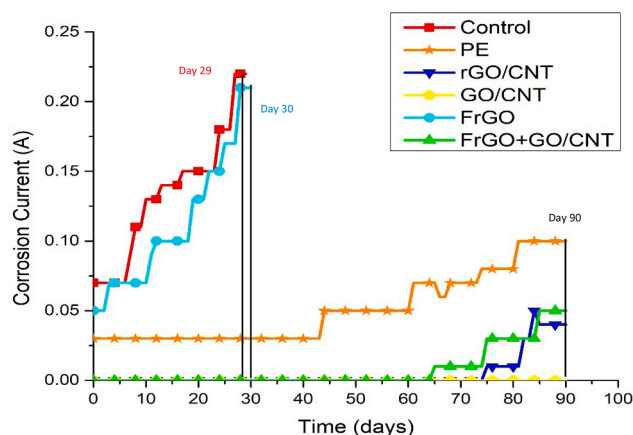


Fig. 15. Variation in corrosion current of coated rebars embedded in concrete.

conductive layer of FrGO without epoxy present beneath the GO/CNT coating. From the corrosion current behavior, it can be concluded that in the FrGO + GO/CNT dual coating the rate of corrosion is lower but corrosion in the early stages initiates in the lower FrGO coating without epoxy, although its progression rate is very slow as compared to the PE coated rebars.

3.3.2. Coated rebars embedded in concrete

The coated rebars cast in concrete were subjected to accelerated corrosion at constant voltage of 15 V for 90 days to investigate the efficacy of modification of the ECR with graphene modifiers in concrete. The corresponding variation in the corrosion current with increase in corrosion was recorded and is presented in Fig. 15. It is generally observed that the corrosion current trends in bars embedded in concrete are in exact coherence with bars tested without concrete in Section 3.3.1. In the **control rebar** concrete specimen, a first sudden jump in corrosion current was observed after 7–8 days indicating initiation of corrosion. The bar gave way in 29 days when a maximum current of 0.22A was observed and its ultrasonic signals had completely vanished. Similar trends and behavior were observed in the FrGO bars without epoxy (Fig. 15).

On the other hand, in the **PE coated rebars** concrete samples, corrosion initiation and progression was very slow and corrosion current depicted a minor increase from 0.03 A to 0.05A on 45th day indicating initiation of corrosion which was also confirmed visually as accumulation of the corrosion product near the cross-section ends. After 90 days of accelerated corrosion, current in PE samples reached to 0.1A as against 0.22A (two times) in 29 days for the control rebar concrete specimens.

In the **rGO/CNT coated rebar** concrete specimens, corrosion initiation was observed after 75 days. The corrosion current observed at 90

Table 2  
Summary of corrosion initiation in differently coated rebars.

Coating	Initiation of corrosion (days) Coated rebars		Initiation of corrosion (days) Coated rebars embedded in Concrete	
	Visual Observation	Corrosion Current	Visual Observation	Corrosion Current
Control	1	1	7–10	7
PE	6–7	6–7	25–35	40–45
rGO/CNT	28–30	36–40	50–60	70–75
GO/CNT	Never initiated	Never initiated	Never initiated	Never initiated
FrGO	1	1	8–10	4–10
FrGO + GO/CNT	5–7	20–25	45–50	60–65

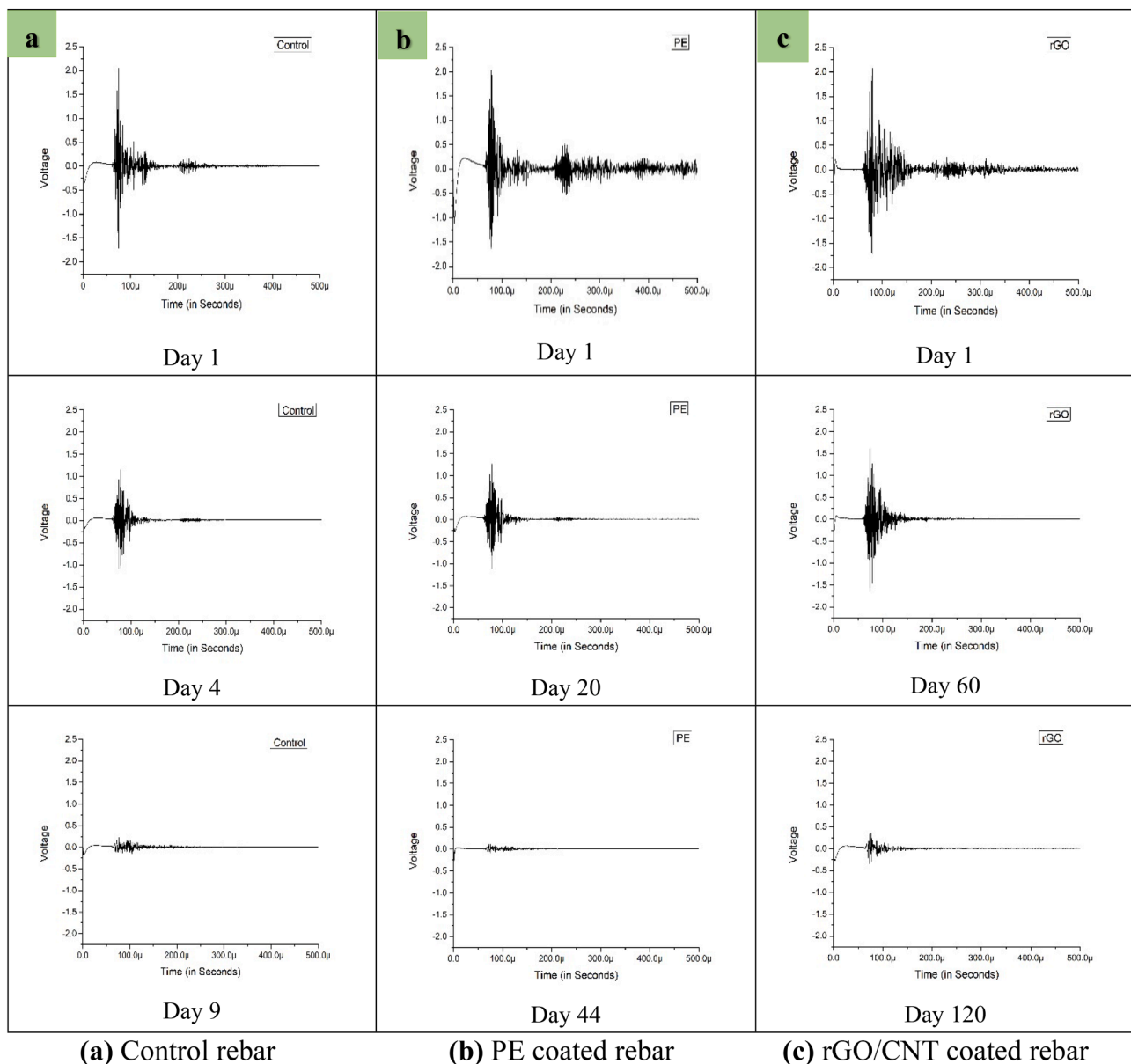


Fig. 16. Ultrasonic signatures at different phases of accelerated corrosion in coated rebars.

days was 0.04A as against 0.1A (two times) in the PE concrete samples. However, in the *GO/CNT coated rebar* concrete specimens no change in corrosion current was noticed after 90 days, validating the visual observation of the concrete specimens and indicating there was no initiation of corrosion in the GO/CNT concrete specimens. In a twin coated *FrGO + GO/CNT* rebar, increase in corrosion current (0A to 0.01A) was observed after 60–65 days, which reached to 0.05A after 90 days of accelerated corrosion.

Both the visual observations and corrosion current measurements support each other as far as corrosion initiation is concerned (Table 2). However, among the coated rebar samples, in the *FrGO + GO/CNT* coated rebars, their visual observations indicated more deterioration than observed in the corrosion current values where no rise was observed till 20–25 days. For the coated rebars embedded in concrete, more divergence between the visual and current measurements is observed. Hence, for quantitative estimation of corrosion, corrosion current measurements need to be supplemented with another NDT parameter to investigate the efficacy of different coatings for corrosion protection. In this work, ultrasonic guided wave monitoring has been

used to supplement and support quantification of corrosion [82–84,93].

### 3.4. Ultrasonic guided wave monitoring

Ultrasonic guided wave approach is generally deployed for non-destructive measurement of initiation and progression during accelerated corrosion. For ultrasonic guided wave evaluation, differently coated samples were removed from power supply and monitored using the set-up shown in Fig. 4. The ultrasonic signals transmitted through rebars are measured. In healthy condition of rebars, ultrasonic signals have highest peak to peak voltage of 3.7 V–3.8 V. With corrosion progression in rebar, the ultrasonic guided wave signal drops due to pitting and area reduction in rebar as a result of accelerated corrosion. Throughout the accelerated corrosion testing ultrasonic signatures were captured for each rebar sample every 24 h. The corresponding variation in ultrasonic guided wave was assessed with increase in corrosion.

#### 3.4.1. Coated rebars

Ultrasonic signatures at three different phases of the accelerated

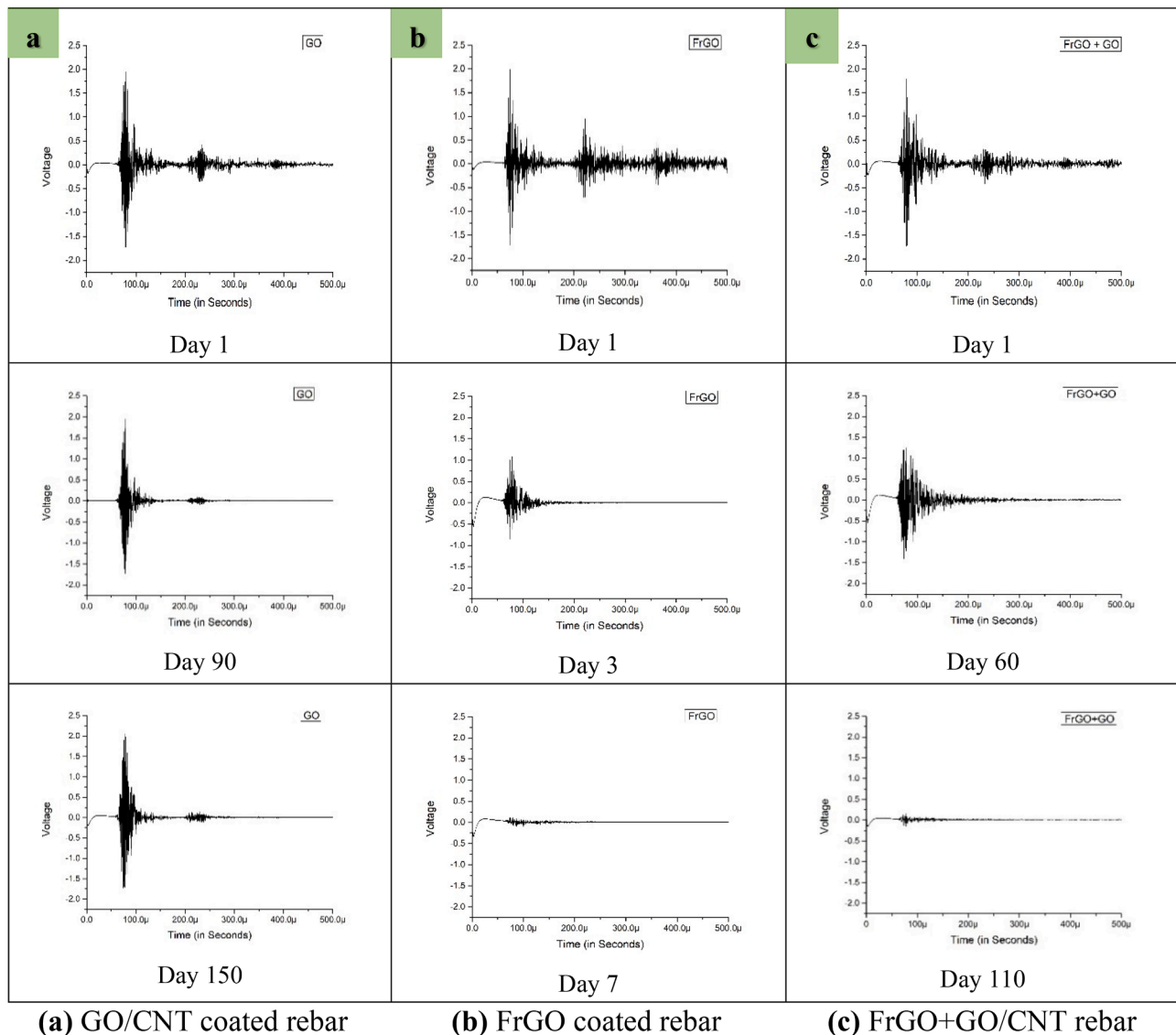


Fig. 17. Ultrasonic signatures at different phases of accelerated corrosion in coated rebars.

corrosion testing for the control rebar and differently coated rebars are shown in Fig. 16 and Fig. 17. From ultrasonic signatures, the peak-to-peak voltage of the received signals for the bars with increasing corrosion is plotted in Fig. 18 as a ratio of that for the healthy rebar. As the corrosion increases or coating gives way to aggressive media, the rebar start losing its material in the form of rust; pitting initiates and the guided wave signal strength starts decreasing since the guided wave travelling through the rebar experiences scattering and mode conversions as it interacts with the pits leading to drop in signals.

From the ultrasonic signatures shown in Figs. 16 and 17, it can be observed that initially all rebars have highest signal amplitude which depletes with increasing corrosion level. In *control rebars*, there is a consistent drop in the peak-to-peak voltage ratio right from Day 1 and finally the signal vanishes in 9 days (Figs. 18 and 16a). The *FrGO coated rebars*, without epoxy, behave in a similar way to control bars and ultrasonic signals completely vanish in 7 days pointing to the ineffectiveness of FrGO without epoxy in corrosion inhibition (Fig. 17b). On the other hand, in the *PE coated rebars*, the signal could sustain for 44 days (Fig. 16b) as against 9 days in the uncoated bar. Corrosion initiates after 8 days in the PE bar as indicated by the first drop in the peak-to-peak voltage ratio, which continuously falls and depletes completely (Fig. 18). It is important to mention that the rate of fall of the peak-to-

peak voltage ratio in the PE rebars is moderate as compared to the control rebar, indicating better performance.

On the other hand, in the *rGO/CNT coated rebars*, the bar was able to hold corrosion for 125 days as against 9 and 44 days in the control and PE coated rebars, respectively. No drop in the voltage ratio was observed till 47 days (Fig. 18), but once corrosion initiated, a consistent and significant drop in signal was observed until the signal completely vanished in 125 days. Also the rate of drop of ultrasonic signals is much lower than in the PE coated rebars (pointing towards better inhibition offered by addition of rGO and CNT in epoxy in ECR bars).

In the *GO/CNT coated rebars*, no drop in ultrasonic signal amplitude was observed even after 150 days (Fig. 17a and Fig. 18) of accelerated corrosion. These results are in complete coherence with the corrosion current measurements. The GO/CNT coated rebars were able to stop corrosion from occurring all together. No initiation was picked up either visually, or by an increase in corrosion current or by a drop in ultrasonic guided wave signals pointing towards the superior and better corrosion inhibition as against the rGO/CNT coated rebars.

The *FrGO + GO/CNT coated rebars* encountered a drop in the ultrasonic signals after 34 days, which is faster as compared to the rGO/CNT coated rebars due to the inner FrGO layer without epoxy. The rate of deterioration follows similar trend (slightly better) than the rGO/CNT

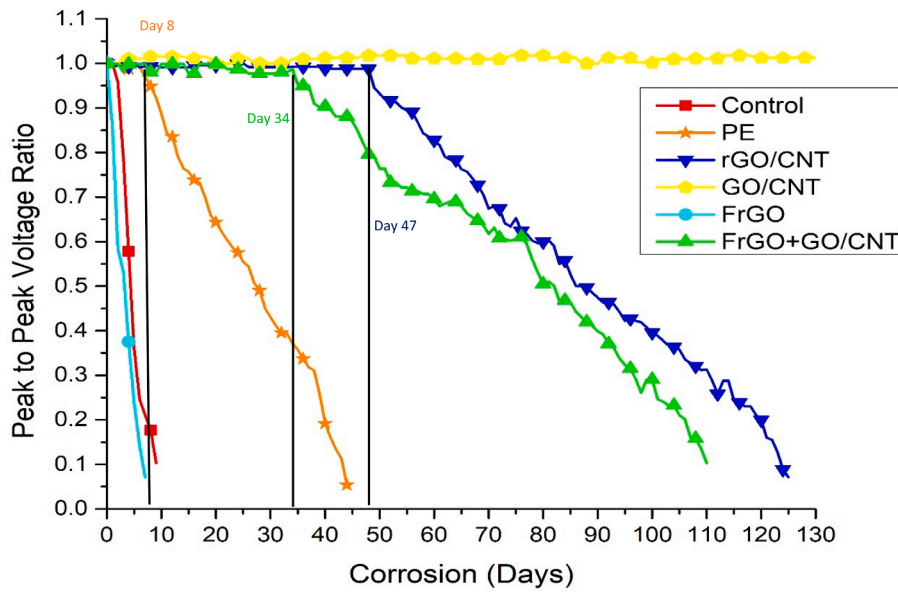


Fig. 18. Peak to peak voltage ratio of rebars only with increasing corrosion.

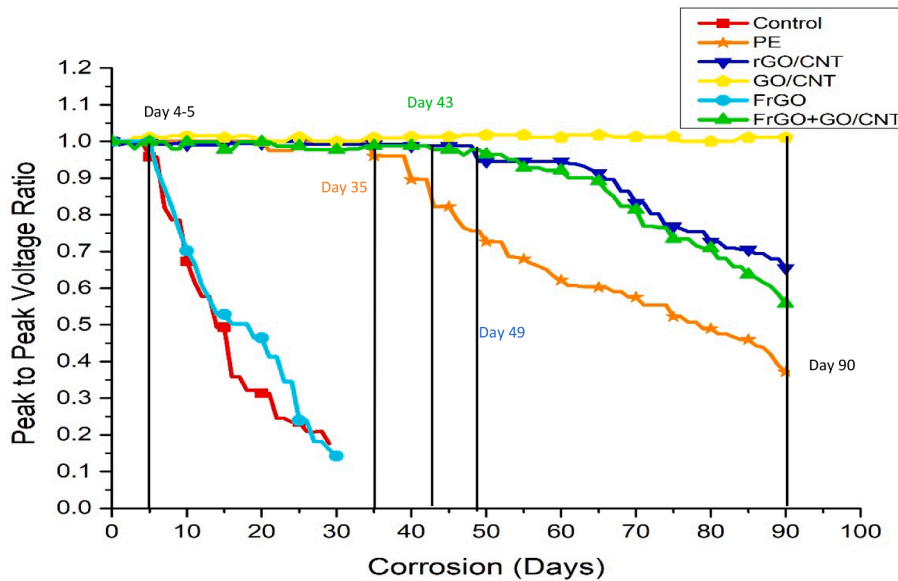


Fig. 19. Peak to peak voltage ratio of rebar embedded in concrete with increasing corrosion.

bars due to outer layer of GO.

Hence, it can be concluded that the GO/CNT modified epoxy coating performs best indicating that epoxy coatings modified with GO/CNT form a dense, impenetrable layer on rebars which does not give way at all in comparison to the rGO/CNT coated rebars in which corrosion initiation as well as progression is observed.

### 3.4.2. Coated rebars embedded in concrete

Ultrasonic guided wave signal amplitudes with increasing corrosion in coated rebars in concrete follow similar trends as in plain bars without concrete (Fig. 19). In the **control rebar** concrete specimen, ultrasonic signals start falling after 4–5 days and completely vanishes in 29 days. However, in the **PE coated rebars** concrete samples, initial drop in ultrasonic signals is observed after 35 days whereas corrosion current increase was observed after 45 days (Fig. 15), indicating superior effectiveness of ultrasonic guided wave monitoring in picking up bar deterioration due to corrosion. At 90 days, the voltage ratio in PE bar is

still 0.37 as against 0.10 value reached in plain bar in 29 days.

In the **rGO/CNT coated rebar** concrete specimens, drop in ultrasonic signals was observed after 49 days as against 35 days in the PE concrete samples. After 90 days of accelerated corrosion, its peak-to-peak ratio is high (0.65) in comparison to PE bars (0.37) indicating better corrosion inhibition. However, in the **GO/CNT coated rebar** concrete samples no drop in signals was observed after 90 days of accelerated corrosion whereas in the rGO/CNT coated rebars in concrete specimens are not able to stop corrosion from occurring all together.

In the **FrGO + GO/CNT coated bars** in concrete, drop is observed at 43 days as against 49 days in rGO/CNT concrete samples pointing towards the less effectiveness of FrGO + GO/CNT coating than rGO/CNT coating. Overall, it can be concluded that GO/CNT nano-composite modified coatings on ECRs are most effective in corrosion inhibition in reinforced concrete specimens as confirmed by visual, corrosion current and ultrasonic guided wave measurements.



Fig. 20. Condition of healthy rebar, corroded control rebar and GO/CNT coated rebar.



Fig. 21. Corroded rebars with different coatings.

### 3.5. Destructive testing

Destructive testing of the extracted bars after corrosion was done to evaluate the mass loss and residual tensile strength for quantitative investigation of corrosion extent and to relate to non-destructive corrosion current and ultrasonic guided wave results. After the completion of a specific duration, differently coated corroded rebars were removed or extracted from the concrete sample and cleaned with

iron brush and acetone to remove the corrosion products on the rebar.

#### 3.5.1. Visual condition of rebars

Healthy rebar, control rebar and GO/CNT coated rebar cleaned after corrosion exposure are presented in Fig. 20. It can be observed that in control rebar reduction in diameter of rebar due to pitting of corrosion was almost uniform throughout the length with approximate residual diameter of 8–9 mm as compared to the original 12 mm diameter. In the

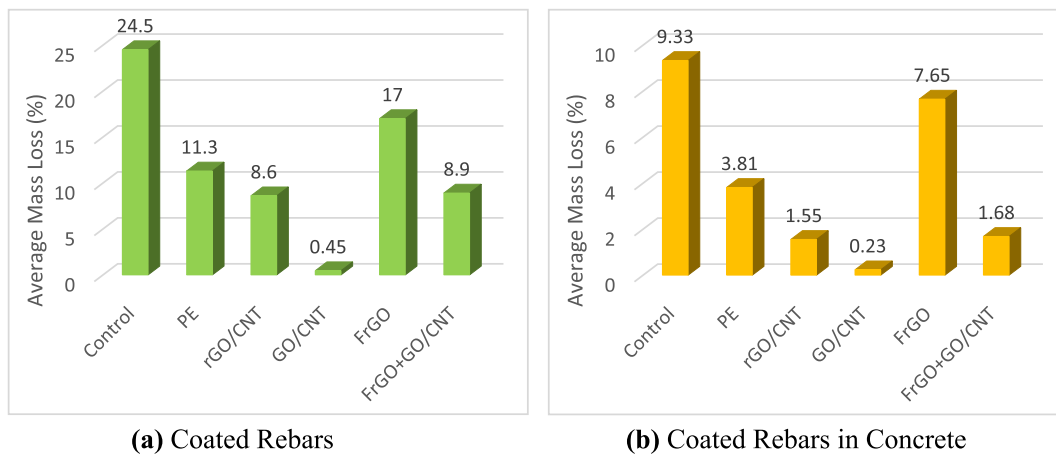


Fig. 22. Average mass loss (%) of corroded rebars.

GO/CNT coated rebar, the coating was intact with no visual damage due to corrosion to the region subjected to accelerated corrosion. But the projected ends of this rebar which were uncoated and subjected to surrounding aggressive environment experienced minor degradation. From Fig. 21 it can be observed that, in the PE coated rebars, a deep pit was observed at one place with multiple pits throughout the extracted bar.

In the rGO/CNT extracted rebar deep pits were observed as in PE rebars except that the pits were less and did not spread widely as in the PE rebar. However, in the FrGO rebar reduction in diameter was non-uniform as compared to the control rebar. This may be due to introduction of rGO which inhibits corrosion but the entire length of rebar faces corrosion pitting since there is no epoxy in the FrGO rebar coat. In FrGO + GO/CNT rebars, several corrosion spots which were noticed in visual inspection got converted into deep pits as corrosion progressed. Entire rebar was affected by the corrosion degradation with very deep pits at some places.

Cleaned rebars were weighed to evaluate their mass loss after corrosion. These extracted rebars were then subjected to tensile testing in UTM to determine residual tensile strength to quantify corrosion loss.

### 3.5.2. Mass loss

Average mass loss experienced by corroded control rebar samples was 24.5% in comparison to the healthy rebar (Fig. 22a). By comparison, the mass loss experienced by differently coated rebars of PE, rGO/CNT, GO/CNT was 11.3%, 8.6%, 0.45%, respectively relative to healthy rebar weight. In functionalized rGO samples, it was 17% and 8.9% in FrGO and FrGO + GO/CNT, respectively.

Introduction of pure epoxy effectively reduces corrosion by approximately 53% in comparison to the control/uncoated rebar. However, the rGO/CNT coated rebars are 65% more efficient than the control rebar and 24% more efficient in comparison to the PE coated rebars in terms of mass loss experienced. No major mass loss is experienced by GO/CNT coated rebars and they remain uncorroded till 150 days. A minor mass loss of 0.45% observed in GO/CNT rebar due to the erosion experienced on the uncoated projected ends of rebar indicating almost 100% efficiency of GO/CNT coated rebars in comparison with all other rebars.

In the FrGO rebars, the mass loss experienced is highest in comparison to other coated rebars except control/uncoated rebars, indicating again their ineffectiveness without epoxy. The FrGO + GO/CNT coated rebar performs better than PE and has 21% more efficacy in comparison with PE rebars since inner layer of FrGO without epoxy is ineffective and leads to early initiation of corrosion.

An upshot of all these results is that out of graphene derivatives of rGO and GO, GO/CNT coatings are the best performing modified epoxy coatings for corrosion inhibition, as indicated by the data for non-destructive corrosion current, ultrasonic guided waves measurements, and by mass loss measurements. It is due to the presence of functional groups on basal planes in GO sheets, which leads to better bonding with epoxy and provides defect free coatings. Further, CNT incorporation of carbon nanotubes leads to an impenetrable layer on rebars and blocks the entry of aggressive chloride ions inside. On the other hand, in rGO/CNT coatings, rGO though hydrophobic leads to delayed initiation and further progression into rebars in comparison with pure epoxy coating but not as much effective as GO/CNT coated rebars. Similar encouraging

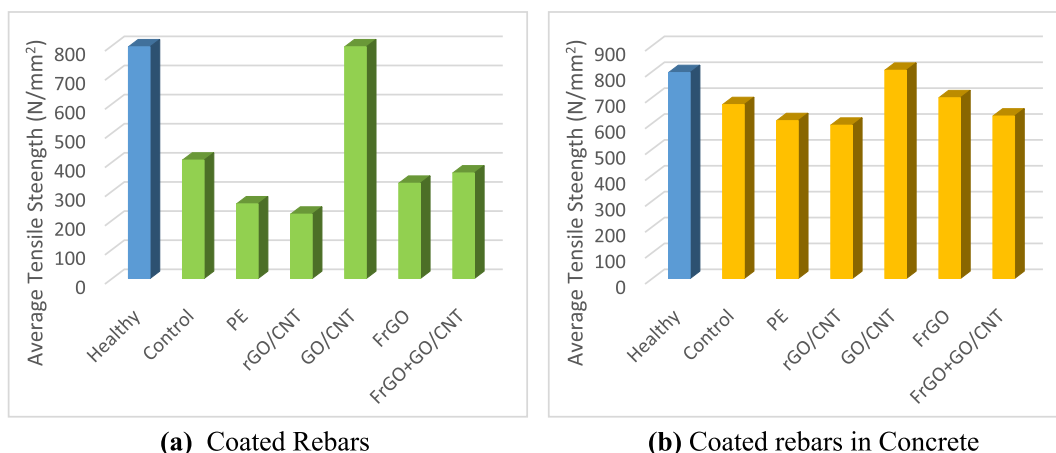


Fig. 23. Average residual tensile strength of the corroded rebars.

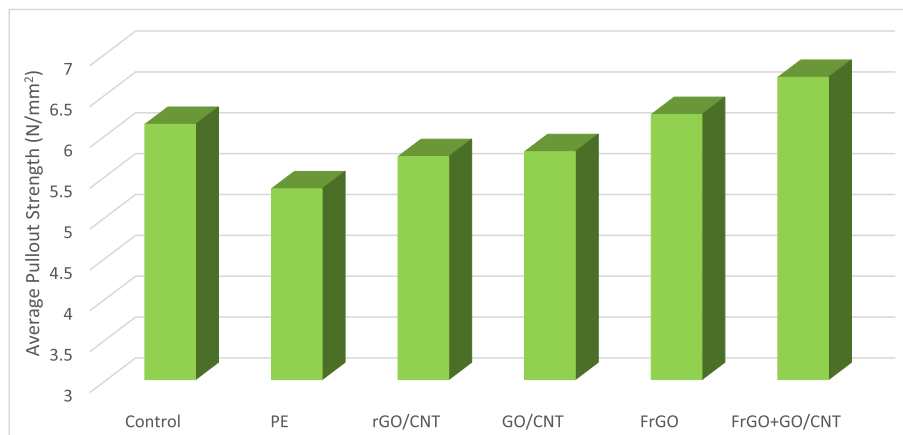


Fig. 24. Average pullout strength of rebars in cylinder.

results were obtained for the corroded samples extracted from the concrete subjected to 90 days accelerated corrosion at 15 V (Fig. 22b).

### 3.5.3. Residual tensile strength

In further affirmation of the results, all the corroded rebars samples as well as extracted rebars from concrete were tested to evaluate residual tensile strength (Fig. 23a). Due to the pitting and dissolution of metal from the rebars, a loss in residual strength is observed for all corroded rebars. An interesting observation is that the residual tensile strength of control rebar is 48% less and for PE coated samples it increases to 67% (Fig. 23a). This is possibly due to the uniform corrosion experienced by uncoated rebars and presence of uneven localized large pits in PE rebars leading to stress concentration points (Figs. 20 and 21).

Similar large drop in tensile strength of 70% was observed in the rGO/CNT coated rebars due to deep localized pits. Residual tensile strength of the FrGO and FrGO + GO/CNT coated rebars reduced by 58% and 54%, respectively due to multiple corrosion spots but no deep pits.

As expected, no drop in tensile strength is observed with the GO/CNT coated rebars since they experienced no deterioration during the entire corrosion exposure. Similarly, bars extracted from concrete matched the results observed for the coated rebars (Fig. 23b).

From non-destructive testing of corrosion current and ultrasonic guided waves and destructive testing of mass loss and residual tensile strength results, it can be concluded that out of different graphene derivatives used in the study GO/CNT modified epoxy coatings did not give way at all and performed the best whereas rGO/CNT modified experienced degradation. GO/CNT reported no corrosion spots in visual inspection, no increase in corrosion current no voltage drop during guided wave monitoring and reported highest residual tensile strength and lowest mass loss. For rebars in concrete as in RC structures, this study suggests the modification of epoxy in small proportion by GO along with CNT as against rGO/CNT for corrosion inhibition in ECR. CNT adds to the better dispersion and reinforce graphene derivatives and provides mechanical strength to epoxy coatings.

The destructive testing results of mass loss and residual tensile strength validate non-destructive corrosion current and ultrasonic guided wave measurements indicating their efficacy for picking up corrosion degradation in RC structures.

### 3.6. Pull-out strength

Finally, for completeness of work, concrete cylinders (Section 2.6.2) with control rebar and coated rebars were subjected to pullout strength testing in uncorroded condition to evaluate their bond strength with surrounding concrete. The pull out strength experienced by each rebar is represented in Fig. 24. As indicated there, pull-out strength of the PE

coated rebars is lowest among all other samples since pure epoxy introduced glassy and very smooth surface. In the rGO/CNT and GO/CNT coated rebars, pull out strength was close to the control rebar. With the introduction of graphene derivatives, rGO and GO with CNTs, the surface texture of coatings is relatively rough in comparison to that for pure epoxy, resulting in relatively higher pullout strength.

On the other hand, pullout strength of the FrGO rebars is similar to that for the control rebar samples due to the absence of epoxy. Further, in the FrGO + GO/CNT coated rebars, pullout strength recorded is slightly more than that for even the control rebar. This is because the surface is very rough and can also be noticed in the prepared sample (Fig. 2). It may be due to the introduction of the base coat of FrGO without epoxy, which makes top surface uneven resulting in irregular surface finish.

From the pullout strength, it can be noticed that the degree of variation in all the coated rebars is not significant but modification by GO/CNT and rGO/CNT causes little improvement in bond strength as compared to pure epoxy coatings. Hence, nano-modification of epoxy in ECR by graphene derivatives not only enhances corrosion inhibition capabilities but also improves the bond strength.

## 4. Conclusions

In the present study, the efficacy and efficiency of epoxy coated rebars modified with graphene derivatives of GO and rGO are investigated for the corrosion protection of reinforcing steel. The degree of inhibition offered by different coatings and their performance was evaluated by qualitative visual inspection, quantitative indicators of non-destructive parameters of corrosion current and ultrasonic guided waves, and destructive parameters of mass loss and loss in tensile strength (Section 3). The following main conclusions are derived from this study:

- Rebars with epoxy coatings modified by graphene derivatives of rGO and GO with CNTs form a dense, impermeable and durable coating when compared to pure epoxy coatings vis-s-vis corrosion inhibition capabilities. Plain epoxy coated rebars only hold corrosion initiation by 7–8 days as against 40–50 days in rGO/CNT coated bars, as indicated by an increase in the corrosion current and a drop in guided wave signal. No change altogether in corrosion current and guided wave signal voltage in GO/CNT bars is observed throughout the accelerated corrosion exposure (No initiation).
- Plain epoxy coated rebars could effectively hold corrosion till 44 days when guided wave signals vanish completely as against 125 days in the rGO/CNT coated bars. No drop in the guided wave signal and increase in corrosion current was observed in GO/CNT coated rebars even after 150 days of corrosion exposure.

**Table 3**

A comprehensive comparison of corrosion initiation and progression in coated rebars.

Coating	Composition of coating	Initiation of corrosion (days)	Withstand accelerated corrosion exposure (days)
Control	Uncoated rebar	1 day	9 days
FrGO	Functionalized rGO in silane solution with no epoxy	1 day	7 days
PE	Pure epoxy coating	7–8 days	44 days
FrGO + GO/CNT	Base coat of functionalized rGO in silane solution and top coat of epoxy coating modified with GO, CNT and silane agents	30–40 days	110 days
rGO/CNT	Epoxy coating modified with rGO, CNT and silane agents	40–50 days	125 days
GO/CNT	Epoxy coating modified with GO, CNT and silane agents	No initiation even after 150 days	Holds for more than 150 days easily and still continuing

- Millions of nano particles in the form of graphene derivatives of rGO and GO along with CNTs in the epoxy matrix offer tortuous paths for diffusion of the aggressive media. The presence of functional groups on the surface of GO sheets traps the aggressive ions within its network whereas highly hydrophobic nature of rGO leads to better corrosion protection than PE coatings.
- Non-destructive testing results of corrosion current and ultrasonic guided wave monitoring are well validated and corroborated by destructive tests of mass loss and residual tensile strength of corroded coated samples. The rebars coated with PE and rGO/CNT respectively experienced comparable mass loss (11.3% and 8.6%) and loss in tensile strength (67% and 70%). On the other hand, the GO/CNT samples experienced marginal mass loss (0.45%) due to minor corrosion at the ends and practically no drop in tensile strength.
- Similar encouraging and repeatable non-destructive as well as destructive results were obtained in nano-modified coated rebars when embedded in concrete utilizing graphene derivatives.
- Epoxy modified with GO/CNT offers a superior coating as compared to rGO/CNT for long term corrosion protection of RC structures in aggressive chloride corrosion environment as in marine conditions. This is because, GO is successful in blocking the entry of aggressive larger chloride ions which are responsible for breakdown of the passive layer of oxides on rebars, which initiates corrosion. It provides a dense impenetrable network due to the presence of functional groups on basal planes of GO sheets. rGO offers short term protection due to its hydrophobicity but its conductive nature compromises the long term protection to corrosion.
- The modification of epoxy by graphene derivatives of rGO and GO added to the bond strength with surrounding concrete as compared to pure epoxy coating. Hence, modifications in ECR would enhance the load carrying capacity in RC structures.
- Table 3 represents the vis-à-vis comparison of performance of differently coated rebars in terms of initiation and progression of corrosion of coated rebars as recorded in this study.
- Finally, the modification of epoxy by graphene derivatives of rGO and GO added to the bond strength with surrounding concrete as compared to pure epoxy coating. Hence, modifications in ECR would enhance the load carrying capacity in RC structures.

We believe that these results would have great impact in the terms of increasing safety and overall service life of RC structures by drastically cutting down repair and maintenance costs.

## Declaration of Competing Interest

The authors declare that they have no known competing financial interests or personal relationships that could have appeared to influence the work reported in this paper.

## Acknowledgements

The research is funded by CEEMS (Centre for Excellence in Emerging Materials), TIET, Patiala and is duly acknowledged.

## References

- [1] G. Koch, J. Varney, N. Thompson, O. Moghissi, M. Gould, J. Payer, *International Measures of Prevention, Application, and Economics of Corrosion Technologies Study*, NACE, International (2016).
- [2] Koch, G. H. *Historic Congressional Study: Corrosion Costs and Preventive Strategies in the United States*. 2002.
- [3] Z.J. Chen, Effect of reinforcement corrosion on the serviceability of reinforced concrete structures, in: *Civil Engineering*, Dundee, Scotland, 2004.
- [4] J.P. Broomfield, *Corrosion of Steel in Concrete: Understanding, investigation and repair*, E&FN Spon (2007).
- [5] Y. Chen, C. Xia, Z. Shepard, N. Smith, N. Rice, A.M. Peterson, A. Sakulich, Self-healing coatings for steel-reinforced concrete, *ACS Sustainable Chemistry & Engineering* 5 (5) (2017) 3955–3962.
- [6] K. Sakr, Effect of cement type on the corrosion of reinforcing steel bars exposed to acidic media using electrochemical techniques, *Cem. Concr. Res.* 35 (9) (2005) 1820–1826.
- [7] K.Y. Yeau, E.K. Kim, An experimental study on corrosion resistance of concrete with ground granulate blast-furnace slag, *Cem. Concr. Res.* 35 (7) (2005) 1391–1399.
- [8] J. Xu, L. Jiang, J. Wang, Influence of detection methods on chloride threshold value for the corrosion of steel reinforcement, *Constr. Build. Mater.* 23 (5) (2009) 1902–1908.
- [9] Farhan, N. A., Sheikh, M. N., & Hadi, M. N. (2018, June). Experimental investigation on the effect of corrosion on the bond between reinforcing steel bars and fibre reinforced geopolymer concrete. In *Structures* (Vol. 14, pp. 251–261). Elsevier.
- [10] B. Dong, W. Ding, S. Qin, N. Han, G. Fang, Y. Liu, F. Xing, S. Hong, Chemical self-healing system with novel microcapsules for corrosion inhibition of rebar in concrete, *Cement and Concrete Composites* 85 (2018) 83–91.
- [11] X. Wang, F. Xing, M. Zhang, N. Han, Z. Qian, Experimental study on cementitious composites embedded with organic microcapsules, *Materials* 6 (9) (2013) 4064–4081.
- [12] K. Van Tittelboom, N. De Belie, Self-healing in cementitious materials—A review, *Materials* 6 (6) (2013) 2182–2217.
- [13] A.R. Boğa, İ.B. Topçu, Influence of fly ash on corrosion resistance and chloride ion permeability of concrete, *Construction and Building Materials* 31 (2012) 258–264.
- [14] S. Kakooei, H.M. Akil, A. Dolati, J. Rouhi, The corrosion investigation of rebar embedded in the fibers reinforced concrete, *Construction and Building Materials* 35 (2012) 564–570.
- [15] A.H. Korayem, P. Ghoddousi, A.S. Javid, M.A. Oraie, H. Ashegh, Graphene oxide for surface treatment of concrete: A novel method to protect concrete, *Construction and Building Materials* 243 (2020), 118229.
- [16] X. Pan, Z. Shi, C. Shi, T.-C. Ling, N. Li, A review on surface treatment for concrete—Part 2: Performance, *Construction and Building Materials* 133 (2017) 81–90.
- [17] D.M. Kim, H.C. Yu, H.I. Yang, Y.J. Cho, K.M. Lee, C.M. Chung, Microcapsule-type self-healing protective coating for cementitious composites with secondary crack preventing ability, *Materials* 10 (2) (2017) 114.
- [18] H.-I. Yang, D.-M. Kim, H.-C. Yu, C.-M. Chung, Microcapsule-type organogel-based self-healing system having secondary damage preventing capability, *ACS applied materials & interfaces* 8 (17) (2016) 11070–11075.
- [19] Y.-K. Song, Y.-H. Jo, Y.-J. Lim, S.-Y. Cho, H.-C. Yu, B.-C. Ryu, S.-I. Lee, C.-M. Chung, Sunlight-induced self-healing of a microcapsule-type protective coating, *ACS applied materials & interfaces* 5 (4) (2013) 1378–1384.
- [20] K. Kaur, S. Goyal, B. Bhattacharjee, M. Kumar, Electrochemical Impedance Spectroscopy to study the carbonation behavior of concrete treated with corrosion inhibitors, *Journal of Advanced Concrete Technology* 15 (12) (2017) 738–748.
- [21] K. Kaur, S. Goyal, B. Bhattacharjee, M. Kumar, Efficiency of migratory-type organic corrosion inhibitors in carbonated environment, *Journal of advanced concrete technology* 14 (9) (2016) 548–558.
- [22] J.O. Okeniyi, C10H18N2Na2O10 inhibition and adsorption mechanism on concrete steel-reinforcement corrosion in corrosive environments, *Journal of the Association of Arab Universities for Basic and Applied Sciences* 20 (1) (2016) 39–48.
- [23] V.T. Ngala, C.L. Page, M.M. Page, Corrosion inhibitor systems for remedial treatment of reinforced concrete. Part 2: sodium monofluorophosphate, *Corrosion Science* 45 (7) (2003) 1523–1537.
- [24] X.-H. Wang, Y. Gao, Corrosion behavior of epoxy-coated reinforced bars in RC test specimens subjected to pre-exposure loading and wetting-drying cycles, *Construction and Building Materials* 119 (2016) 185–205.

- [25] ShiGang Dong, B. Zhao, ChangJian Lin, RongGui Du, RongGang Hu, G.X. Zhang, Corrosion behavior of epoxy/zinc duplex coated rebar embedded in concrete in ocean environment, *Construction and building materials* 28 (1) (2012) 72–78.
- [26] H. Binici, H. Zengin, G. Zengin, F. Yasarer, The use of pumice as a coating for the reinforcement of steel against corrosion and concrete abrasions, *Corrosion science* 50 (8) (2008) 2140–2148.
- [27] Ş. Erdogdu, T.W. Bremner, L.L. Kondratova, Accelerated testing of plain and epoxy-coated reinforcement in simulated seawater and chloride solutions, *Cement and Concrete Research* 31 (6) (2001) 861–867.
- [28] A.A. Sagiés, H.M. Perez-Duran, R.G. Powers, Corrosion performance of epoxy-coated reinforcing steel in marine substructure service, *Corrosion* 47 (11) (1991) 884–893.
- [29] X.-H. Wang, B. Chen, P. Tang, Experimental and analytical study on bond strength of normal uncoated and epoxy-coated reinforcing bars, *Construction and Building Materials* 189 (2018) 612–628.
- [30] A. Ramniceanu, R.E. Weyers, J.S. Riffle, M.M. Sprinkel, Parameters governing corrosion protection efficacy of fusion-bonded epoxy coatings on reinforcing bar, *ACI Materials Journal* 105 (5) (2008) 459.
- [31] Z. Zhou, P. Qiao, Bond behavior of epoxy-coated rebar in ultra-high performance concrete, *Construction and Building Materials* 182 (2018) 406–417.
- [32] J.J. Assaad, C.A. Issa, Bond strength of epoxy-coated bars in underwater concrete, *Construction and Building Materials* 30 (2012) 667–674.
- [33] J.J. Chang, W. Yeih, C.L. Tsai, Enhancement of bond strength for epoxy-coated rebar using river sand, *Construction and Building Materials* 16 (8) (2002) 465–472.
- [34] M.A. Alam, U.A. Samad, E.S.M. Sherif, A.M. Poulouse, J.A. Mohammed, N. Alharthi, S.M. Al-Zahrani, Influence of SiO<sub>2</sub> content and exposure periods on the anticorrosion behavior of epoxy nanocomposite coatings, *Coatings* 10 (2) (2020) 118.
- [35] N. Sharma, S. Sharma, S.K. Sharma, R. Mehta, Evaluation of corrosion inhibition and self-healing capabilities of nanoclay and tung oil microencapsulated epoxy coatings on rebars in concrete, *Construction and Building Materials* 259 (2020) 120278, <https://doi.org/10.1016/j.conbuildmat.2020.120278>.
- [36] A.M. Motlatle, S.S. Ray, M. Scriba, Polyaniline-clay composite-containing epoxy coating with enhanced corrosion protection and mechanical properties, *Synthetic Metals* 245 (2018) 102–110.
- [37] H. Pulikkalparambil, S. Siengchin, J. Parameswaranpillai, Corrosion protective self-healing epoxy resin coatings based on inhibitor and polymeric healing agents encapsulated in organic and inorganic micro and nanocontainers, *Nano-structures & nano-objects* 16 (2018) 381–395.
- [38] A. Weishaar, M. Carpenter, R. Loucks, A. Sakulich, A.M. Peterson, Evaluation of self-healing epoxy coatings for steel reinforcement, *Construction and Building Materials* 191 (2018) 125–135.
- [39] R. Yuan, H. Liu, P. Yu, H. Wang, J. Liu, Enhancement of adhesion, mechanical strength and anti-corrosion by multilayer superhydrophobic coating embedded electroactive PANI/CNF nanocomposite, *Journal of Polymer Research* 25 (7) (2018) 151.
- [40] F.T. Shirehjini, I. Danaee, H. Eskandari, D. Zarei, Effect of nano clay on corrosion protection of zinc-rich epoxy coatings on steel 37, *Journal of Materials Science & Technology* 32 (11) (2016) 1152–1160.
- [41] E. Matin, M.M. Attar, B. Ramezanzadeh, Investigation of corrosion protection properties of an epoxy nanocomposite loaded with polysiloxane surface modified nanosilica particles on the steel substrate, *Progress in Organic Coatings* 78 (2015) 395–403.
- [42] S. Pour-Ali, C. Dehghanian, A. Kosari, Corrosion protection of the reinforcing steels in chloride-laden concrete environment through epoxy/polyaniline-camphorsulfonate nanocomposite coating, *Corrosion Science* 90 (2015) 239–247.
- [43] A.H. Navarchian, M. Joulazadeh, F. Karimi, Investigation of corrosion protection performance of epoxy coatings modified by polyaniline/clay nanocomposites on steel surfaces, *Progress in Organic Coatings* 77 (2) (2014) 347–353.
- [44] M. Karimi Sahnesarayi, H. Sarpoolaky, S. Rastegari, Effect of heat treatment temperature on the performance of nano-TiO<sub>2</sub> coating in protecting 316L stainless steel against corrosion under UV illumination and dark conditions, *Surface and Coatings Technology* 258 (2014) 861–870.
- [45] A.A. Azeez, K.Y. Rhee, S.J. Park, D. Hui, Epoxy clay nanocomposites—processing, properties and applications: A review, *Composites Part B: Engineering* 45 (1) (2013) 308–320.
- [46] B. Ramezanzadeh, M.M. Attar, Studying the corrosion resistance and hydrolytic degradation of an epoxy coating containing ZnO nanoparticles, *Materials Chemistry and Physics* 130 (3) (2011) 1208–1219.
- [47] K.M. Aujara, B.W. Chieng, N.A. Ibrahim, N. Zainuddin, C. Thevy Ratnam, Gamma-irradiation induced functionalization of graphene oxide with organosilanes, *International journal of molecular sciences* 20 (8) (2019) 1910.
- [48] C.-H. Jung, J.-H. Hong, J.-M. Jung, I.-T. Hwang, C.-H. Jung, J.-H. Choi, Preparation of sulfonated reduced graphene oxide by radiation-induced chemical reduction of sulfonated graphene oxide, *Carbon letters* 16 (1) (2015) 41–44.
- [49] Bianco, A., Cheng, H. M., Enoki, T., Gogotsi, Y., Hurt, R. H., Koratkar, N., ... & Zhang, J. (2013). All in the graphene family—a recommended nomenclature for two-dimensional carbon materials.
- [50] S.-Y. Lee, R.L. Mahajan, A Facile Method for Coal to Graphene Oxide and its Application to a Biosensor, *Carbon* 181 (2021) 408–420.
- [51] W. Sun, L. Wang, T. Wu, Y. Pan, G. Liu, Synthesis of low-electrical-conductivity graphene/pernigraniline composites and their application in corrosion protection, *Carbon* 79 (2014) 605–614.
- [52] A. Krishnamurthy, V. Gadhamshetty, R. Mukherjee, Z. Chen, W. Ren, H.-M. Cheng, N. Koratkar, Passivation of microbial corrosion using a graphene coating, *Carbon* 56 (2013) 45–49.
- [53] W. Zheng, W.G. Chen, T. Feng, W.Q. Li, X.T. Liu, L.L. Dong, Y.Q. Fu, Enhancing chloride ion penetration resistance into concrete by using graphene oxide reinforced waterborne epoxy coating, *Progress in Organic Coatings* 138 (2020) 105389, <https://doi.org/10.1016/j.porgcoat.2019.105389>.
- [54] S. Amrollahi, B. Ramezanzadeh, H. Yari, M. Ramezanzadeh, M. Mahdavian, Synthesis of polyaniline-modified graphene oxide for obtaining a high performance epoxy nanocomposite film with excellent UV blocking/anti-oxidant/anti-corrosion capabilities, *Composites Part B: Engineering* 173 (2019), 106804.
- [55] W. Sun, T. Wu, L. Wang, Z. Yang, T. Zhu, C. Dong, G. Liu, The role of graphene loading on the corrosion-promotion activity of graphene/epoxy nanocomposite coatings, *Composites Part B: Engineering* 173 (2019), 106916.
- [56] S. Zhou, Y. Wu, W. Zhao, J. Yu, F. Jiang, Y. Wu, L. Ma, Designing reduced graphene oxide/zinc rich epoxy composite coatings for improving the anticorrosion performance of carbon steel substrate, *Materials & Design* 169 (2019) 107694, <https://doi.org/10.1016/j.matdes.2019.107694>.
- [57] J. Liu, Q. Yu, M. Yu, S. Li, K. Zhao, B. Xue, H. Zu, Silane modification of titanium dioxide-decorated graphene oxide nanocomposite for enhancing anticorrosion performance of epoxy coatings on AA-2024, *Journal of Alloys and Compounds* 744 (2018) 728–739.
- [58] S. Zhou, Y. Wu, W. Zhao, J. Yu, F. Jiang, L. Ma, Comparative corrosion resistance of graphene sheets with different structures in waterborne epoxy coatings, *Colloids and Surfaces A: Physicochemical and Engineering Aspects* 556 (2018) 273–283.
- [59] F.A. Ghauri, M.A. Raza, M.S. Baig, S. Ibrahim, Corrosion study of the graphene oxide and reduced graphene oxide-based epoxy coatings, *Materials Research Express* 4 (12) (2017) 125601, <https://doi.org/10.1088/2053-1591/aa9aac>.
- [60] N. Parhizkar, T. Shahrazi, B. Ramezanzadeh, A new approach for enhancement of the corrosion protection properties and interfacial adhesion bonds between the epoxy coating and steel substrate through surface treatment by covalently modified amino functionalized graphene oxide film, *Corrosion science* 123 (2017) 55–75.
- [61] H. Zheng, Y. Shao, Y. Wang, G. Meng, B. Liu, Reinforcing the corrosion protection property of epoxy coating by using graphene oxide-poly (urea-formaldehyde) composites, *Corrosion Science* 123 (2017) 267–277.
- [62] A.B. Ikhe, A.B. Kale, J. Jeong, M.J. Reece, S.-H. Choi, M. Pyo, Perfluorinated polysiloxane hybridized with graphene oxide for corrosion inhibition of AZ31 magnesium alloy, *Corrosion Science* 109 (2016) 238–245.
- [63] M. Mo, W. Zhao, Z. Chen, E. Liu, Q. Xue, Corrosion inhibition of functional graphene reinforced polyurethane nanocomposite coatings with regular textures, *Rsc Advances* 6 (10) (2016) 7780–7790.
- [64] B. Ramezanzadeh, S. Niroumandrad, A. Ahmadi, M. Mahdavian, M.H. Moghadam, Enhancement of barrier and corrosion protection performance of an epoxy coating through wet transfer of amino functionalized graphene oxide, *Corrosion Science* 103 (2016) 283–304.
- [65] Y.-P. Hsieh, M. Hofmann, K.-W. Chang, J.G. Jhu, Y.-Y. Li, K.Y. Chen, C.C. Yang, W.-S. Chang, L.-C. Chen, Complete corrosion inhibition through graphene defect passivation, *ACS nano* 8 (1) (2014) 443–448.
- [66] R.K. Gupta, M. Malviya, C. Verma, M.A. Quraishi, Aminoazobenzene and diaminoazobenzene functionalized graphene oxides as novel class of corrosion inhibitors for mild steel: experimental and DFT studies, *Materials Chemistry and Physics* 198 (2017) 360–373.
- [67] Lin, G., Xie, B. H., Hu, J., Huang, X., & Zhang, G. J. (2015). Aligned graphene oxide nanofillers: an approach to prepare highly thermally conductive and electrically insulative transparent polymer composites. *Journal of Nanomaterials*, 2015.
- [68] G. Mittal, V. Dhand, K.Y. Rhee, S.-J. Park, W.R. Lee, A review on carbon nanotubes and graphene as fillers in reinforced polymer nanocomposites, *Journal of Industrial and Engineering Chemistry* 21 (2015) 11–25.
- [69] Y.-H. Yu, Y.-Y. Lin, C.-H. Lin, C.-C. Chan, Y.-C. Huang, High-performance polystyrene/graphene-based nanocomposites with excellent anti-corrosion properties, *Polymer Chemistry* 5 (2) (2014) 535–550.
- [70] K.S. Aneja, H.L.M. Böhm, A.S. Khanna, S. Böhm, Functionalised graphene as a barrier against corrosion, *FlatChem* 1 (2017) 11–19.
- [71] S. Pourhashem, M.R. Vaezi, A. Rashidi, M.R. Bagherzadeh, Distinctive roles of silane coupling agents on the corrosion inhibition performance of graphene oxide in epoxy coatings, *Progress in Organic Coatings* 111 (2017) 47–56.
- [72] A. Ahmadi, B. Ramezanzadeh, M. Mahdavian, Hybrid silane coating reinforced with silanized graphene oxide nanosheets with improved corrosion protective performance, *Rsc Advances* 6 (59) (2016) 54102–54112.
- [73] B. Ramezanzadeh, E. Raeisi, M. Mahdavian, Studying various mixtures of 3-aminopropyltriethoxysilane (APS) and tetraethylorthosilicate (TEOS) silanes on the corrosion resistance of mild steel and adhesion properties of epoxy coating, *International Journal of Adhesion and Adhesives* 63 (2015) 166–176.
- [74] Y.-J. Wan, L.-X. Gong, L.-C. Tang, L.-B. Wu, J.-X. Jiang, Mechanical properties of epoxy composites filled with silane-functionalized graphene oxide, *Composites Part A: Applied Science and Manufacturing* 64 (2014) 79–89.
- [75] R. Aradhana, S. Mohanty, S.K. Nayak, Comparison of mechanical, electrical and thermal properties in graphene oxide and reduced graphene oxide filled epoxy nanocomposite adhesives, *Polymer* 141 (2018) 109–123.
- [76] Yan, Z., Peng, Z., Casillas, G., Lin, J., Xiang, C., Zhou, H., ... & Tour, J. M. (2014). Rebar graphene. *ACS nano*, 8(5), 5061–5068.
- [77] S. Han, Q. Meng, S. Araby, T. Liu, M. Demiral, Mechanical and electrical properties of graphene and carbon nanotube reinforced epoxy adhesives: Experimental and numerical analysis, *Composites Part A: Applied Science and Manufacturing* 120 (2019) 116–126.

- [78] E.F. Hacıoğlu, Y. Yang, B.o. Ni, Y. Li, X. Li, Q. Chen, H. Guo, J.M. Tour, H. Gao, J. Lou, Toughening graphene by integrating carbon nanotubes, *ACS nano* 12 (8) (2018) 7901–7910.
- [79] F.H. Gojny, J. Nastalczyk, Z. Roslaniec, K. Schulte, Surface modified multi-walled carbon nanotubes in CNT/epoxy-composites, *Chemical physics letters* 370 (5-6) (2003) 820–824.
- [80] A. Kausar, I. Rafique, B. Muhammad, Review of applications of polymer/carbon nanotubes and epoxy/CNT composites, *Polymer-Plastics Technology and Engineering* 55 (11) (2016) 1167–1191.
- [81] N. Pal Kaur, J. Kumar Shah, S. Majhi, A. Mukherjee, Healing and simultaneous ultrasonic monitoring of cracks in concrete, *Materials Today Communications* 18 (2019) 87–99.
- [82] A. Sharma, S. Sharma, S. Sharma, A. Mukherjee, Monitoring invisible corrosion in concrete using a combination of wave propagation techniques, *Cement and Concrete Composites* 90 (2018) 89–99.
- [83] A. Sharma, S. Sharma, S. Sharma, A. Mukherjee, Investigation of deterioration in corroding reinforced concrete beams using active and passive techniques, *Construction and Building Materials* 161 (2018) 555–569.
- [84] S. Sharma, A. Mukherjee, Nondestructive evaluation of corrosion in varying environments using guided waves, *Research in Nondestructive Evaluation* 24 (2) (2013) 63–88.
- [85] S. Sharma, A. Mukherjee, Monitoring corrosion in oxide and chloride environments using ultrasonic guided waves, *Journal of Materials in Civil Engineering* 23 (2) (2011) 207–211.
- [86] B.L. Ervin, D.A. Kuchma, J.T. Bernhard, H. Reis, Monitoring corrosion of rebar embedded in mortar using high-frequency guided ultrasonic waves, *Journal of engineering mechanics* 135 (1) (2009) 9–19.
- [87] N. Nikfar, Y. Zare, K.Y. Rhee, Dependence of mechanical performances of polymer/carbon nanotubes nanocomposites on percolation threshold, *Physica B: Condensed Matter* 533 (2018) 69–75.
- [88] A. Nistal, E. Garcia, D. Pérez -Coll, C. Prieto, M. Belmonte, M.I. Osendi, P. Miranzo, Low percolation threshold in highly conducting graphene nanoplatelets/glass composite coatings, *Carbon* 139 (2018) 556–563.
- [89] D. Zheng, G. Tang, H.-B. Zhang, Z.-Z. Yu, F. Yavari, N. Koratkar, S.-H. Lim, M.-W. Lee, In situ thermal reduction of graphene oxide for high electrical conductivity and low percolation threshold in polyamide 6 nanocomposites, *Composites Science and Technology* 72 (2) (2012) 284–289.
- [90] J.C. Grunlan, A.R. Mehrabi, M.V. Bannon, J.L. Bahr, Water-based single-walled-nanotube-filled polymer composite with an exceptionally low percolation threshold, *Advanced Materials* 16 (2) (2004) 150–153.
- [91] Sharma, N. (2019). Evaluation of Performance of Epoxy Based Coatings for Corrosion Inhibition in Reinforcing Bars (Master's Thesis).
- [92] S. Sharma, A. Mukherjee, Monitoring freshly poured concrete using ultrasonic waves guided through reinforcing bars, *Cement and Concrete Composites* 55 (2015) 337–347.
- [93] S. Sharma, A. Mukherjee, Longitudinal guided waves for monitoring chloride corrosion in reinforcing bars in concrete, *Structural Health Monitoring* 9 (6) (2010) 555–567.